




# The 2020 California fire season: A year like no other, a return to the past or a harbinger of the future?

Hugh D. Safford<sup>1,2,3</sup>  | Alison K. Paulson<sup>2,4</sup>  | Zachary L. Steel<sup>5</sup> |  
Derek J. N. Young<sup>6</sup>  | Rebecca B. Wayman<sup>2</sup>

<sup>1</sup>USDA Forest Service, Pacific Southwest Region, Vallejo, California, USA

<sup>2</sup>Department of Environmental Science and Policy, University of California, Davis, California, USA

<sup>3</sup>Vibrant Planet, Incline Village, Nevada, USA

<sup>4</sup>USDA Forest Service, Humboldt-Toiyabe National Forest, Sparks, Nevada, USA

<sup>5</sup>Department of Environmental Science, Policy, and Management, University of California, Berkeley, Berkeley, California, USA

<sup>6</sup>Department of Plant Sciences, University of California, Davis, California, USA

## Correspondence

Hugh D. Safford, Department of Environmental Science and Policy, University of California, Davis, CA 95616, USA.

Email: [hdsafford@ucdavis.edu](mailto:hdsafford@ucdavis.edu)

**Handling Editor:** Morgan Varner

## Abstract

**Aim:** Wildfire burned area, fire size, fire severity and the ecological and socio-economic impacts of fire have been increasing rapidly in California in recent decades. We summarize the record-breaking 2020 wildfire season in California statistically, evaluate the drivers of high-severity burning in the 2020 fires and consider implications for fire and resource management.

**Location:** California, USA.

**Time period:** 2020, with consideration of long-term trends in many variables.

**Major taxa studied:** Humans, vegetation and wildlife.

**Methods:** We statistically summarize the record-breaking 2020 fire year in California and outline the salient ecological and socio-economic impacts. Then we fit two statistical models to determine how a suite of weather- and fuel-related variables influenced high-severity burning in different vegetation types and in different fire events during the 2020 fire season.

**Results:** In 2020, 1.74 million ha burned in California, 2.2 times more than the previous historical record but only average when compared with pre-Euroamerican conditions. Economic losses exceeded \$19 billion, and 33 people were killed directly by fire. Vegetation type and recent fire history had important effects on burning. Variability in high-severity burning among vegetation types was driven principally by vapour pressure deficit and wind speed; variability among fire events was related principally to time since the last fire (a surrogate for fuel loading).

**Main conclusions:** The 2020 fires were part of an accelerating decades-long trend of increasing burned area, fire size, fire severity and socio-ecological costs in California. In fire-prone forests, the management emphasis on reducing burned area should be replaced by a focus on reducing the severity of burning and restoring key ecosystem functions after fire. There have been positive developments in California vis-à-vis collaborative action and increased pace and scale of fuel management and pre- and postfire restoration, but the warming climate and other factors are rapidly constraining our options.

## KEYWORDS

2020 fires, burned area, California, fire management, fire severity, fire weather, fuels

## 1 | INTRODUCTION

After decades of successful fire suppression, wildfire area and the occurrence of large wildfires have been increasing in California since the late 1980s (Figure 1; Keeley & Syphard, 2021; Miller et al., 2009). The first recorded million-acre (>405,000 ha) year in California was 1999, with six of the following 21 years also surpassing this mark. Including 2021 (we are in the autumn fire season at the time of writing), 4 of the last 5 years have burned >405,000 ha, and the mean annual area burned over the same period is >900,000 ha (Figure 1). Nonetheless, after a series of staggering fire years [2017 and 2018 killed 147 people, destroyed almost 35,000 homes and businesses and resulted in c. \$34 billion in insured economic losses (2020 \$)], 2019 was a whimper of a fire year, with only 105,000 ha burned and <750 structures lost (Safford et al., 2021; <https://www.fire.ca.gov/stats-events/>; <http://iii.org>).

Perhaps 2019 lulled people to sleep or we fell prey to wishful thinking. But somehow 2020 seemed to catch Californians by surprise; 2020 was a record year for wildfire in California, with 1.74 million ha burned in the state, more than doubling the previous documented record for annual area burned set in 2018 (0.8 million ha). Once again, thousands of structures were burned and dozens of people lost their lives. Between August and November, it was hard to breath in most of the state. A lot has been written about the 2020 California fire year in government reports, in the media and on the Internet. The primary focus of these accounts has been on the magnitude of the wildfire events, the heroics of fire fighters and the plights of the people and communities affected. Given

that the events are only a year past, the scientific literature specific to the 2020 fire season is much thinner and has centred thus far on the roles of climate and weather (Higuera & Abatzoglou, 2020; Son et al., 2021), the health effects of wildfire smoke (Navarro & Vaidyanathan, 2020; Zhou et al., 2021) and the historical context of the fire events (Keeley & Syphard, 2021).

In contrast, many scientific studies have examined wildfire trends in California and the neighbouring western USA over the last 20–100 years. The pattern is clear: fires are getting bigger and burning more intensely (Littell et al., 2009; Safford et al., 2021; Steel et al., 2018), and we probably should not be surprised by a year like 2020. But there is a debate about what is driving these trends and why 2020 was so big. Much of the recent literature focuses on the role of climate change in driving fire trends, and California has warmed notably in recent decades: the dry season has expanded, snowpack has receded, and the number and duration of drought events have increased (State of California, 2018). At the same time, burning has increased dramatically in forest-dominated northern California, where a century of fire exclusion has choked forests with live and dead fuels (Safford et al., 2021; Steel et al., 2015), but remained relatively steady in chaparral-dominated southern California, where the most profound climate warming has occurred (State of California, 2018; Figure 1 inset). Other factors are also at play, including mass bark beetle-driven tree mortality events, expansion of other mortality agents, such as *Phytophthora ramorum* (the pathogen causing sudden oak death), invasion of highly flammable exotic grasses, and even changing fire management tactics (Safford et al., 2021).

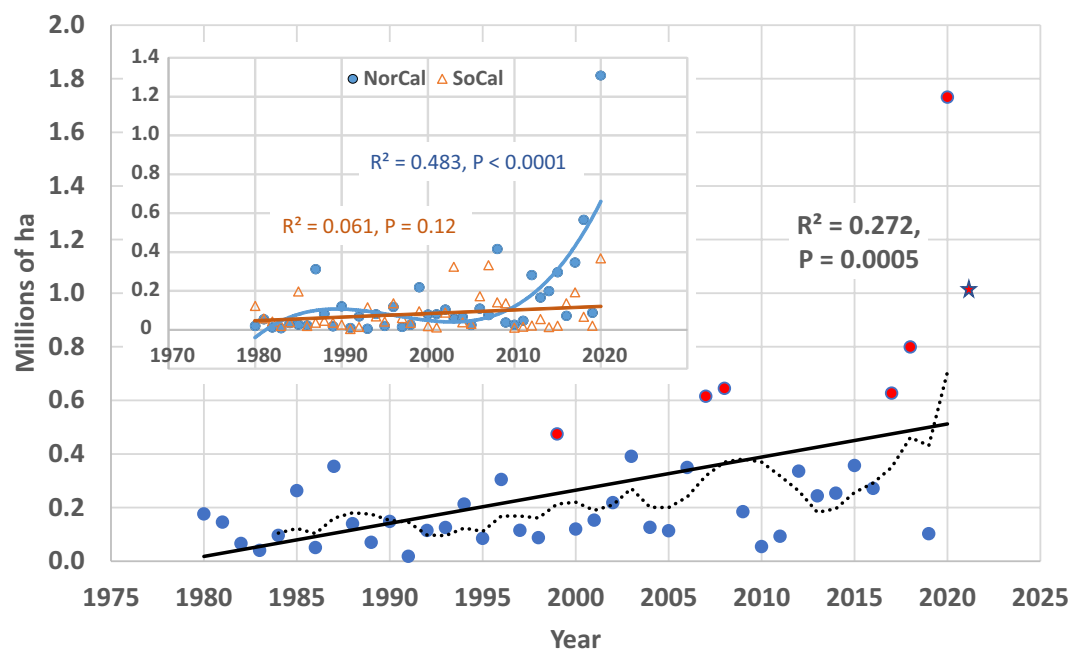


**FIGURE 1** Trend in area burned by wildfires in California, 1980–2020. Data are from CALFIRE (see main text). The dotted line represents the 5-year running mean. Red circles denote years with >405,000 ha (1,000,000 acres) burned. The red star indicates the area burned in 2021 as of 1 December (not included in the regression). Inset: Annual burned area 1980–2020 in northern California (blue) versus southern California (orange; defined as Coast Ranges south of Monterey plus all lands south of the northern boundary of the Transverse Ranges)

Sociopolitical, management and scientific interest in modern wildfire trends tends to focus heavily on a single component of the fire regime: burned area. Burned area is easily measured; records of burned area go back to the first half of the 20th century in much of the USA, and burned area is an easy variable to understand. The principal measure of success in US wildfire management has long been the reduction of burned area. The regional drivers of burned area (or related variables, such as the incidence of large wildfire events) are also relatively well understood, with climate variables (precipitation, air and ocean temperatures, drought severity etc.) directly or indirectly explaining much of the variance, both today and in the past (e.g., Littell et al., 2009; Wahl et al., 2019; Westerling et al., 2006).

An important question is whether burned area warrants so much attention (Kolden, 2020; Miller et al., 2009; Moreira et al., 2020). In the Great Basin and much of coastal and lowland California, where woodlands and shrublands are besieged by highly flammable invasive plants and/or rampant human ignitions, reduction of burned area is a worthy goal. And in moist and higher-elevation forests it might be as well (Mallek et al., 2013; Noss et al., 2006). However, the bulk of the US “wildfire problem” is centred not in these ecosystems but in the fire-prone low- and middle-elevation forestlands that dominate much of the western USA, ecosystems that experienced highly frequent fires before the arrival of Euroamericans and the imposition of fire exclusion policies (Agee, 1993; van Wagtenonk et al., 2018). Today, these forests have experienced a massive fire deficit for a century (Marlon et al., 2012; Stephens et al., 2007), with concomitant increases in stand densities and live and dead fuels that are leading to huge areas of severe burning that threaten ecological function, biodiversity, ecosystem services and human health and safety. In these ecosystems, reduction of burned area is a principal cause of the current trends in fire severity and destructiveness, not a solution to them.

In this contribution, we have two main goals. First, we provide a wide-ranging summary of the record-breaking 2020 fire year in California; we consider the ecological and socio-economic impacts of the fire year, and we put the seemingly extraordinary numbers in historical and longer-term context. Second, in the interest of focusing more on the ecological outcomes of the 2020 fires rather than on their area, we evaluate the patterns and principal drivers of fire severity (a measure of the ecosystem impact of fire, here defined in terms of tree mortality) in 2020. Given that we treat so many different phenomena and types of data, we combine our Results and Discussion, and we finish with a Conclusion centred on the broad management applications of our findings.

## 2 | MATERIALS AND METHODS

### 2.1 | Study area

California is the third largest state in the USA, at 424,000 km<sup>2</sup>. Elevations range from -86 m at Death Valley to >4,400 m in the Sierra Nevada; annual precipitation ranges from 40 mm in desert valleys to

>3,000 mm in the western Klamath Mountains, and seasonal mean temperatures range from January lows of <-12°C in high mountain basins to July highs of >45°C in the desert south-east. About two-thirds of California falls within the North American Mediterranean Climate Zone (NAMCZ; also known as the California Floristic Province), with the rest of the state split among the high volcanic tablelands of the Modoc Plateau (often included in the NAMCZ), the semi-arid Great Basin and the Mojave and Sonoran Deserts (Figure 2).

The climate of the NAMCZ is characterized by warm to hot, dry summers and cool, wet winters. As Safford et al. (2021) note, “most of [California] receives sufficient precipitation in the winter and early spring to produce a crop of fuel just in time for the hot, dry summer”. As a result, California is the most fire-prone state in the USA, and it also supports the most fire-adapted vegetation (Safford et al., 2021; Van Wagtenonk et al., 2018). Fire-prone vegetation in the NAMCZ is characterized primarily by sclerophyllous shrublands (e.g., chaparral and sage scrub), oak-dominated woodlands and conifer-dominated forests with a broadleaf component at low to moderate elevations. Large grassland areas are common in drier interior landscapes, and meadows are widespread in the montane zone.

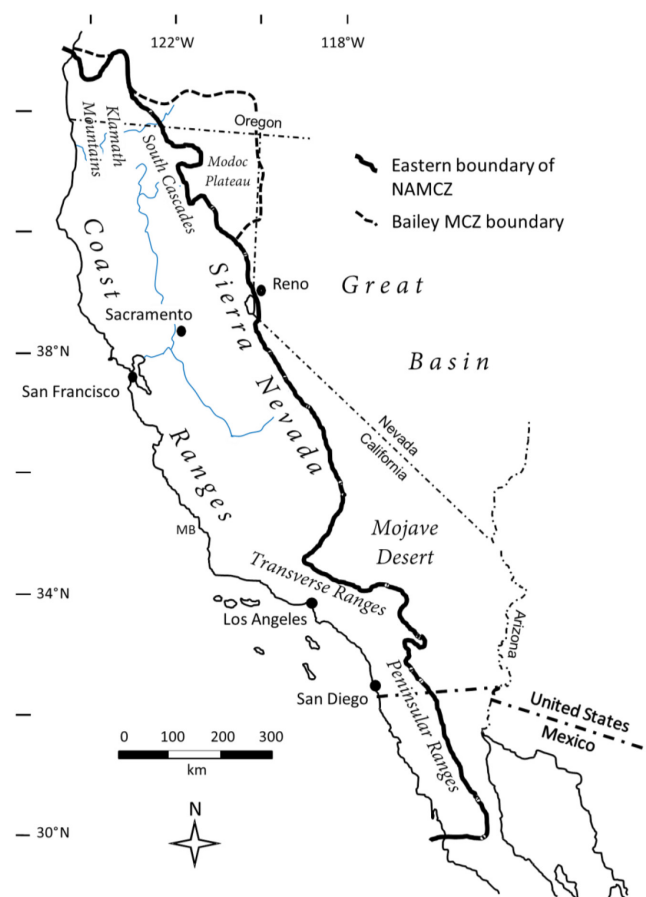


FIGURE 2 California, with major geographical features identified. The North American Mediterranean Climate Zone (NAMCZ) boundary is approximated by the limits of the California Floristic Province; Bailey's (1995) Mediterranean Climate Zone (MCZ) is identical to the NAMCZ except that it includes the Modoc Plateau. Map modified from Safford et al. (2021)

Modern fire regimes have been greatly altered by fire exclusion policies, especially in northern and central Californian forests and woodlands at low and middle elevations, where frequent, primarily low-severity fire was common before Euroamerican settlement ("pre-EAS") (Safford et al., 2021). Some semi-arid shrubland ecosystems in California have suffered the opposite fate, with modern fire regimes often supporting notably more fire than was common pre-EAS. In central and southern California, this is primarily attributable to anthropogenic ignitions in and around urban areas. In contrast, increasing fire frequencies in Great Basin shrublands are attributable to increased fine fuel continuity because of grass invasion. The same dynamic is also affecting some desert areas (Safford et al., 2021; Van Wagtenonk et al., 2018).

## 2.2 | Statistical summary of 2020 fires

We first summarized the burning conditions, spatial extent and socio-economic impact of the fire season by fire for fires that burned >10,000 ha (see Table 1). We downloaded 2020 fire perimeter data and burn date, fire weather, modelled fuel moisture, fatality, property damage and suppression cost data from public data sources (see Supporting Information Appendix S1). The data included records of "red flag days", which are declared by the National Oceanic and Atmospheric Administration National Weather Service (NWS) during critical combinations of low relative humidity and high winds and/or when dry lightning is predicted (for criteria, see: <https://www.weather.gov/gjt/firewxcriteria>).

We then summarized vegetation types and fire history for 2020 fires >10,000 ha (Table 2). Fire return interval departure (FRID) measures, in years, the difference between modern (since 1908) fire frequencies and estimated pre-EAS fire frequencies by presettlement fire regime (PFR) type (Safford & Van de Water, 2014; Van de Water & Safford, 2011). The PFRID is the percentage departure of modern fire frequencies from estimated pre-EAS frequencies. The following variables were derived by overlaying fire perimeters on the California FRID database (<https://www.fs.usda.gov/detail/r5/landmanagement/gis/>): dominant potential vegetation types (based on PFR); percentage of fire area occupied by each vegetation type; percentage of fire area previously burned and unburned; area-weighted mean time since last fire (TSLF; with the different TSLF values weighted by their area within the fire perimeter); and area-weighted mean PFRID. We identify in the text when further sources were consulted. We also collected data on geographical areas, size, cause and duration; structures and lives lost; and suppression costs for all 2020 wildfires between 405 (1,000 acres) and 10,000 ha. These are listed in the Supporting Information (Table S1).

## 2.3 | Fire severity analysis of 2020 fires

### 2.3.1 | Fire selection and fire severity

We extracted the 40 largest 2020 fire perimeters (all >2,420 ha) from the California Fire Perimeter Database (<https://frap.fire.ca.gov/>

[frap-projects/fire-perimeters/](https://frap-projects/fire-perimeters/); accessed 7 May 2021). The final sample size for this analysis was 38 owing to imagery, location and fire perimeter constraints with two smaller fires (Mountain View and Bond). We used initial assessments (Key & Benson, 2006) of the relative differenced normalized burn ratio (RdNBR; Miller & Thode, 2007) to estimate fire severity (extended assessments are not available until  $\geq 1$  year after the fire). Given that fire-caused tree mortality continues for some time (Miller et al., 2016), our fire severity estimates are likely to be lower than estimates made with 1-year postfire data, but the overall difference in accuracy between the two methods is low (Lydersen et al., 2016; Miller & Quayle, 2015). We obtained 30-m resolution RdNBR estimates for our fires from the US Forest Service (USFS) Rapid Assessment of Vegetation Condition After Wildfire (RAVG; <https://fsapps.nwcg.gov/ravg/>) and from a modification to the Google Earth Engine approach developed by Parks et al. (2018) (Supporting Information Appendix S1).

We considered any pixel with an initial RdNBR severity estimate  $\geq 641$  as "high-severity fire" (Lydersen et al., 2016), corresponding to a composite burn index of 2.25–3.0 (Key & Benson, 2006) and an approximate field-measured basal area mortality in yellow pine and mixed conifer ("YPMC") forest types of 95–100% (Lydersen et al., 2016). Thresholds relating initial RdNBR assessments to field-based estimates of fire severity in shrubland ecosystems have yet to be developed; hence, our estimates of the extent of high-severity burning in shrublands might be less accurate.

### 2.3.2 | Inferring burn date and fire weather

We obtained the date of burning for each 30-m pixel within each fire perimeter by spatially interpolating between satellite thermal anomaly ("hotspot") point detections using the "weighted by mean and distance" method of Parks (2014) (Supporting Information Appendix S1).

We estimated fire weather by extracting c. 4-km resolution gridMET weather data (Abatzoglou, 2013; <http://www.climatologylab.org/gridmet.html>) occurring within each 30 m pixel on the associated burn date using bilinear interpolation. We selected vapour pressure deficit (VPD; in kilopascals) and wind speed (in metres per second) to represent immediate fire weather, and we selected modelled 1,000-h fuel moisture (as a percentage) to capture longer-term moisture conditions more related to seasonal aridity. The 1,000-h fuels correspond to "coarse woody debris" (branches and logs >7.6 cm in diameter), which are not present in all the vegetation types we evaluated. However, we included this term in order to account for the important seasonal/lagged weather effect often observed in systems with coarse fuels (van Wagtenonk, 2018), with the expectation that this predictor would have less influence in vegetation types lacking substantial large-diameter fuels.

### 2.3.3 | Extracting biophysical data

In addition to fire weather, our models incorporated information about time since the last fire (TSLF; in years), drought mortality and

vegetation type. To approximate fuel levels and recent fire history, we used TSLF from the 2019 FRID Database (see above). Pixels with higher TSLF are likely to have increased fuel loadings (Steel et al., 2015). An additional source of fuel loading in 2020 in the Sierra Nevada was extensive tree mortality resulting from the 2012–2016 drought and associated bark beetle outbreaks (Stephens et al., 2018; Young et al., 2020). We estimated mortality using the USFS Aerial Detection Monitoring surveys from 2012–2016, in which aerial observers denote polygons with observed tree mortality ([https://www.fs.usda.gov/detail/r5/forest-grasslandhealth/?cxml:id=fsbde v3\\_046696](https://www.fs.usda.gov/detail/r5/forest-grasslandhealth/?cxml:id=fsbde v3_046696); Supporting Information Appendix S1).

To account for variation in fire severity attributable to vegetation type, we obtained California Wildlife Habitat Relationship System (CWHR) vegetation types from the Forest Service Existing Vegetation dataset (EVeg; <https://data.fs.usda.gov/geodata/edw/datasets.php>). In this analysis, we used CWHR instead of PFR because the FRID database does not cover the Californian deserts or portions of the central Coast Ranges and because CWHR types are “existing vegetation” and therefore capture successional changes attributable to disturbance, which can be important for fire behaviour. We lumped similar CWHR types into 14 “CWHR groups” that were correlated closely with the PFR types.

For statistical summarization and modelling purposes, we created a 90-m grid across each burned area and extracted each variable at each grid point. For TSLF, mortality and vegetation type, we extracted the point value for each grid point. We used bilinear interpolation to extract RdNBR fire severity estimates and fire weather. For our fire severity  $\times$  vegetation type tabular and graphical summaries, we thinned the dataset to a 180-m grid. For our statistical modelling (see next subsection), we removed the majority of the fine-scale spatial autocorrelation in our dataset by thinning the 90-m point grid by a factor of 10 to yield a 900-m grid (*sensu* Kane et al., 2015; Supporting Information Appendix S1; Figure S1).

### 2.3.4 | Statistical analysis

We fitted two statistical models to assess the influence of TSLF, drought mortality, VPD, windspeed and 1,000-h fuel moisture on the likelihood of a location burning at high severity: (1) a fire model, and (2) a vegetation model. Both models included fixed effects for all five environmental predictor variables. For the fire model, we assessed how these predictors differed among fires by allowing slope parameters to vary by fire identity (ID) as random effects; in the vegetation model, slope parameters varied by vegetation type. Both models included random intercepts for fire ID and vegetation type to account, in part, for spatial clustering of sample points, but varying slopes with respect to fire and vegetation were modelled separately to avoid confounding parameter estimates. Model response variables were binary, indicating whether a sample location burned at high severity. Models were fitted using a Bernoulli error structure and a logit link. Continuous predictor variables were standardized with a mean of zero and standard deviation of one. Models

were fitted using the brms and rstan packages (Bürkner, 2017; Stan Development Team, 2020) in R (R Core Team, 2020). The full model was fitted using rrms default uninformative flat priors for slope parameters and weakly regularizing priors for variance parameters. Models were run with four chains, each for 2,000 samples, with a warm-up of 1,000 samples and 4,000 total post-warm-up samples. Traceplots and R-hat values were assessed for proper mixing and model convergence. Bayes  $R^2$  values for the fire and vegetation models were 0.22 and 0.20, respectively. The derivative dataset used for analyses of fire severity patterns is archived on OSF ([https://osf.io/8mw9e/?view\\_only=66325d85b82d41dab40a231e716aec2e](https://osf.io/8mw9e/?view_only=66325d85b82d41dab40a231e716aec2e)), and the code used for analyses is available at [https://github.com/akpaulson/2020\\_Fires\\_GEB](https://github.com/akpaulson/2020_Fires_GEB).

## 3 | RESULTS AND DISCUSSION

### 3.1 | The 2020 fire year in numbers

9,917 fires were registered in 2020, with a total burned area of c. 1.74 million ha, 4.2% of the surface area of California. This is 2.2 times more than the previous historical record, set in 2018; 2020 and 2021 (1.035 million ha; <https://www.fire.ca.gov/incidents/2021/>) together burned more area than the previous 7 years combined and only slightly less than the total burned in the 20 years between 1980 and 1999 (Figure 1). The rapid rise in burned area over recent decades has attracted much attention from the media, federal and state fire management agencies and scientists. However, estimates of pre-EAS burning rates in California suggest that c. 1.8 million ha burned in an average year before 1800 (Stephens et al., 2007); 2020 is thus the first year since reliable records were kept in California (beginning in the early 1900s) when burned area has come anywhere close to this baseline.

Overall economic losses attributable to wildfire in 2020 were estimated at c. \$19 billion, with insured losses of c. \$10 billion (Aon, 2021). Approximately 11,116 structures were destroyed (>50% damaged; K. Kovanda, CALFIRE, pers. comm.), and 33 people lost their lives (CALFIRE Incident Archive; <https://www.fire.ca.gov/incidents/2020/>) (Table 1). Trends in insured economic losses and numbers of destroyed structures were relatively static between 2003 and 2014 (Figure 3), except for blips in 2003 and 2007, which were years of destructive fire outbreaks in southern California (Keeley et al., 2009). Insured economic loss (\$2,020) averaged c. \$0.86 billion between 2003 and 2014, and an average of 908 structures were lost each year (Figure 3). In 2015, there was a change in trends in both variables. Since that year, insured economic losses have averaged \$8.5 billion per year, and an annual average of 8,374 structures have been destroyed (Figure 3).

In addition to economic losses, recent fire seasons in California have been characterized by extraordinary declines in air quality, especially in the northern half of the state (Supporting Information Figure S2). According to CALFIRE (2020), the 2020 fires released nearly 112 million Mg of C and 1.2 million Mg  $PM_{2.5}$  (suspended



TABLE 1 Californian wildfires >10,000 ha in size in 2020, with data on geographical areas, size, cause and duration; number of red flag days and 10-h fuel moisture measurements; structures and lives lost; and suppression costs

Fire	Counties (in order of fire area)	Region	Size (ha)	Cause	Start date	Containment date
August Complex	Trinity, Tehama, Mendocino, Glenn, Lake, Shasta	North Coast Ranges	418,097	Lightning	16 August	12 November
SCU	Santa Clara, Stanislaus, Alameda, San Joaquin	Central Coast Ranges	160,485	Lightning	17 August	1 October
Creek	Fresno, Madera	Sierra Nevada	153,798	Probably lightning	4 October	24 December
North Complex	Plumas, Butte, Yuba	Sierra Nevada	129,060	Lightning	17 August	3 December
Hennessy (LNU)	Napa, Yolo, Solano, Lake	North Coast Ranges	123,624	Lightning	17 August	2 October
Castle (SQF)	Tulare	Sierra Nevada	69,088	Lightning	19 August	15 October
Slater	Siskiyou, Del Norte	Klamaths	63,737	Lightning	8 September	16 November
Red Salmon	Trinity, Humboldt, Siskiyou	Klamaths	58,233	Lightning	27 July	17 November
Dolan	Monterey	Central Coast Ranges	50,416	Unknown	18 August	31 December
Bobcat	Los Angeles	Southern California	46,963	Powerline	6 September	6 October
CZU	Santa Cruz, San Mateo	Central Coast Ranges	35,042	Lightning	16 August	22 September
W-5 Cold Springs	Lassen, Modoc	NE Great Basin	34,339	Lightning	18 August	6 September
Caldwell	Siskiyou, Modoc	South Cascades	32,884	Lightning	22 July	20 August
Glass	Napa, Sonoma	North Coast Ranges	27,321	Unknown	27 September	20 October
Zogg	Shasta, Tehama	North Coast Ranges	22,809	Powerline	27 September	13 October
Walbridge (LNU)	Sonoma	North Coast Ranges	22,352	Lightning	17 August	2 October
River	Monterey	Central Coast Ranges	20,330	Lightning	16 August	4 September
Loyalton	Sierra, Lassen, Plumas	Sierra Nevada	18,915	Lightning	14 August	14 September
Dome	San Bernardino	Desert	17,899	Lightning	15 August	1 September
Apple	Riverside	Southern California	13,445	Human	31 July	18 November
Lake	Los Angeles	Southern California	12,550	Unknown	12 August	28 September
Mineral	Fresno	Central Coast Ranges	12,011	Unknown	13 July	29 July
Sheep	Lassen, Plumas	Sierra Nevada	11,960	Lightning	17 August	9 September
Slink	Alpine, Mono	Sierra Nevada	10,831	Lightning	29 August	8 November

Note: Fires are listed in order of final size. See main text for data sources.

particulate matter  $\leq 2.5$  microns in diameter), >120 times greater than the combined emissions of all Californian cars, trucks and buses in the same year. In 4 of the last 5 years, wildfire smoke episodes in northern California have exposed tens of thousands of people annually to dangerous levels of  $PM_{2.5}$  (Cleland et al., 2020). More than half of the population of California experienced air quality index (AQI) levels of unhealthy, very unhealthy or hazardous for 1 month or more in 2020, and the highest 5 days of average air pollution ever recorded in California were all in 2020 (CALFIRE, 2020). An as yet unpublished study by Stanford researchers (<http://www.g-feed.com/2020/09/indirect-mortality-from-recent.html>) used relationships between increasing  $PM_{2.5}$  concentrations and human mortality rates from the study by Deryugina et al. (2019) to estimate that the extreme wildfire-driven  $PM_{2.5}$  values measured in August and early September in California caused between 1,200 and 3,000 “excess”

deaths among the elderly (age  $\geq 65$  years). This estimate is likely to be an underestimate of all excess mortality because: (1) it ignores mortality rates among younger people; (2) it was not informed by more recent work by Aguilera et al. (2021), which demonstrated that wildfire-source  $PM_{2.5}$  is notably more injurious to human health than standard  $PM_{2.5}$ ; and (3) it does not consider interactions with coronavirus disease 2019 infections (Zhou et al., 2021). Although the 2020 fires generated an extreme level of air pollution, the north-west USA (including northern California) has been experiencing a positive wildfire smoke-driven trend in  $PM_{2.5}$  (c. +2% per year) since at least the late 1980s, in contrast to the general decrease in  $PM_{2.5}$  across the rest of the USA (McClure & Jaffe, 2018).

Twenty-four fires burned >10,000 ha (24,700 acres) in 2020 (Tables 1 and 2), accounting for 90% of burned area (1.566 million ha) in California. An additional 51 fires burned >405 ha (1,000 acres;

Duration (days)	Number of red flag days	Mean 10-h fuel moisture (fire duration)	Minimum 10-h fuel moisture (first 5 days)	Structures destroyed	Lives lost	Suppression cost (\$ millions)	Suppression cost per hectare (\$)
88	19	6.4	4.7	935	1	264.1	631.67
45	10	5.6	3.1	222	0	69.4	432.44
81	2	7	3	856	0	193	1,254.89
108	20	7	3	2,455	16	179	1,386.96
46	10	5	3	1,491	6	94.6	765.22
57	5	5	4	228	0	122.3	1,770.20
68	11	8	2	419	2	55	862.92
112	13	6	4	0	0	111.6	1,916.43
135	4	5.5	3.2	14	0	70	1,388.45
30	4	3.7	3	170	0	100	2,129.35
37	7	6	3	1,490	1	55.9	1,595.22
18	3	5.8	4.5	0	0	10.3	299.95
29	9	6.3	3.9	0	0	34.5	1,049.14
23	3	6	4.1	1,555	0	59.9	2,192.42
16	2	5	3	204	4	31	1,359.12
45	6	8.8	4.2	560	0	See Hennessy	
19	6	7.4	4.3	30	0	24.5	1,205.14
31	7	6	3	35	0	8.2	433.51
17	0	4	2	0	0	2.2	122.91
110	13	6.1	3.4	12	0	56.4	4,194.89
47	3	4.4	3.5	12	0	4	318.72
13	0	4.4	2.9	7	0	25.7	2,139.72
23	5	5	4	26	0	21.6	1,806.03
71	5	4.1	3.8	0	0	15	1,384.94

see Supporting Information Table S1), accounting for a further 7% of 2020 burned area. Of these 75 fires, 59% were caused by humans (arson, vehicles, powerlines, campfires, etc., and unknown causes, which are nearly always human) and 41% by lightning (including one designated as “probably lightning”), but the area burned by lightning-ignited fires in 2020 was more than five times greater than the area burned by human-caused fires [1.403 million ha (84%) vs. 0.270 million ha (16%); Table 1]. This is in contrast to most previous years. For example, in 2019, 84% of burned area in California was caused by humans, and 94% in 2018. Stephens (2005) found that between 1940 and 2000, an average of 64% of burned area on USFS lands in California was caused by humans. Before 2020, the most recent exception to the rule was 2008, when 76% of burned area was attributed to lightning ignitions. In 2020, 65% of the area burned by wildfire in California was ignited by lightning strikes

between 16 and 19 August, during an incursion of unstable tropical air from Tropical Storm Fausto (CALFIRE, 2020); fires that burned a total of 586,000 ha were not ignited by this event. Earlier noteworthy California fire seasons were influenced by similar mass lightning events (e.g., 1977, 1987, 2008), but none of them approached the scale of the 2020 event.

Of the 75 fires >405 ha (Table 1; Supporting Information Table S1), the average time to full containment was 35 days (median = 23 days, SE = 4.09 days). This continues a trend that has seen average fire duration for fires >405 ha increase by c. 80% ( $r^2 = 0.375$ ,  $p < .001$ ) since the early 2000s, from c. 19 days between 2000 and 2004 to >34 days between 2016 and 2020. Eight 2020 fires burned for >3 months (four of these were smaller fires managed for resource benefit by the National Park Service; Table 1). As expected, fire duration was correlated with fire size ( $r = 0.430$ ,

**TABLE 2** Table 1 fires, dominant vegetation composition within the fire perimeter, percentage of fire area previously unburned, mean time since last fire (TSLF) and percentage fire return (PFR) interval departure (PFRID)

Fire	Dominant vegetation (PFR types with >10%)	PFR (% of fire area)	Percentage of chaparral + sage scrub	Previously unburned (%) <sup>†</sup>	Burned in last 10 years (%)	Burned in last 15 years (%)	Burned in last 20 years (%)	Burned in last 30 years (%)	Mean TSLF (area weighted) <sup>‡</sup>	Mean PFRID (area weighted)
Dome	Desert mixed shrub, Joshua tree, grassland	No FRID coverage	0	99.9	0	0.1	0	0	112	No data
River	Mixed evergreen, sage scrub, undefined, chaparral	47, 21, 20, 11	31.7	96.8	0.1	0.1	0.4	0.4	112	74.1
W-5 Cold Springs	Big sagebrush, pinyon-juniper	63, 13	0.1	95.1	0.1	0.7	1	2.3	112	68.8
CZU	Redwood, chaparral	76, 11	13	84	9	9.8	10.3	11.5	112	79.5
Creek	Moist mixed conifer, yellow pine, dry mixed conifer, red fir	22, 18, 17, 12	13.4	76.7	9.3	9.8	9.9	12.4	112	80.4
Sheep	Moist mixed conifer, yellow pine, dry mixed conifer	54, 22, 14	1.7	75.8	1.2	18.4	19.1	19.1	112	85.7
Slater	Mixed evergreen, moist mixed conifer	77, 14	5.7	74.5	7	9.5	9.7	10	112	74.1
Slink	Big sagebrush, moist mixed conifer, pinyon-juniper	32, 19, 13	5.1	73.7	0	0.2	24.9	25.1	112	68.9
Mineral	Oak woodland, sage scrub, chaparral	49, 23, 19	18.5	71.9	23.1	23.4	26.5	26.5	112	78.9
August Complex	Moist mixed conifer, dry mixed conifer, mixed evergreen, chaparral	25, 21, 20, 12	14.2	65.6	4.4	14.2	15.4	16.2	112	71.4
Zogg	Oak woodland, undefined (mostly grassland and agriculture)	44, 40	4.9	64.1	8.4	20.9	20.9	20.9	112	80.4
Glass	Mixed evergreen, chaparral, undefined (mostly grassland and agriculture)	55, 22, 15	22.1	63.5	9	9.4	9.6	12.1	112	74.1
Castle (SQF)	Moist mixed conifer, red fir, montane chaparral, dry mixed conifer, yellow pine	29, 18, 13, 12, 10	17.4	61	9	10.3	28.7	28.8	112	71.4
North Complex	Moist mixed conifer, dry mixed conifer, yellow pine	41, 28, 15	0.6	60.9	3.6	15.2	22.9	23.1	112	85.7
Walbridge (LNU)	Mixed evergreen, chaparral	74, 12	11.6	59.9	0.06	0.12	0.12	0.77	112	74.1



TABLE 2 (Continued)

Fire	Dominant vegetation* (PFR types with >10%)	PFR (% of fire area)	Percentage of chaparral + sage scrub	Previously unburned (%) <sup>†</sup>	Burned in last 10 years (%)	Burned in last 15 years (%)	Burned in last 20 years (%)	Burned in last 30 years (%)	Mean TSLF (area weighted) <sup>‡</sup>	Mean PFRID (area weighted)
Loyalton	Big sagebrush, yellow pine	66, 12	5.6	58.4	0.2	0.2	9.7	19	112	68.8
Caldwell	Big sagebrush, yellow pine, undefined (mostly grassland)	70, 11, 11	0.4	58.1	5.3	11.6	14.7	14.8	112	68.8
SCU	Oak woodland, chaparral, undefined, mixed evergreen	36, 20, 19, 17	28	56.4	2.8	24.3	32.4	35.4	112	74.1
Apple	Chaparral, mixed evergreen, mixed conifer (dry + moist)	54, 16, 14	56.9	42.1	10.2	10.4	11.6	16.1	68	0.0
Bobcat	Chaparral, mixed evergreen, bigcone Douglas-fir	39, 11, 10	48.1	31.9	12.7	12.8	18.2	18.7	66	1.8
Hennessy (LNU)	Chaparral, oak woodland, undefined, mixed evergreen	41, 33, 15, 10	41	28.4	37.8	44.8	50.7	53.6	20	25
Red Salmon	Mixed evergreen, moist mixed conifer	48, 28	8.8	14.9	10.7	19.3	58.7	58.7	20	50.9
Dolan	Chaparral, mixed evergreen	52, 21	60.7	4	0.7	48	79.9	85.6	20	-32.7
Lake	Chaparral	77	82.1	2.2	6.7	6.9	7.3	7.5	95	1.8

Note: Fires are ranked in order of the percentage of fire area that was previously unburned. The blue line between SCU and Apple Fires demarcates Groups 1 and 2 referred to in the text: Group 1 (above the line) contains fires that burned landscapes that were mostly unburned before the 2020 event; Group 2 (below the line) contains fires that burned landscapes that were mostly burned before the 2020 event. See main text for data sources.

\*Mixed evergreen includes Douglas-fir and a suite of associated broadleaf species, including evergreen oaks and tan oak. Chaparral can include a suite of serotinous conifers.

<sup>†</sup>In previous 111 years.

<sup>‡</sup>112 years if no previous fire.

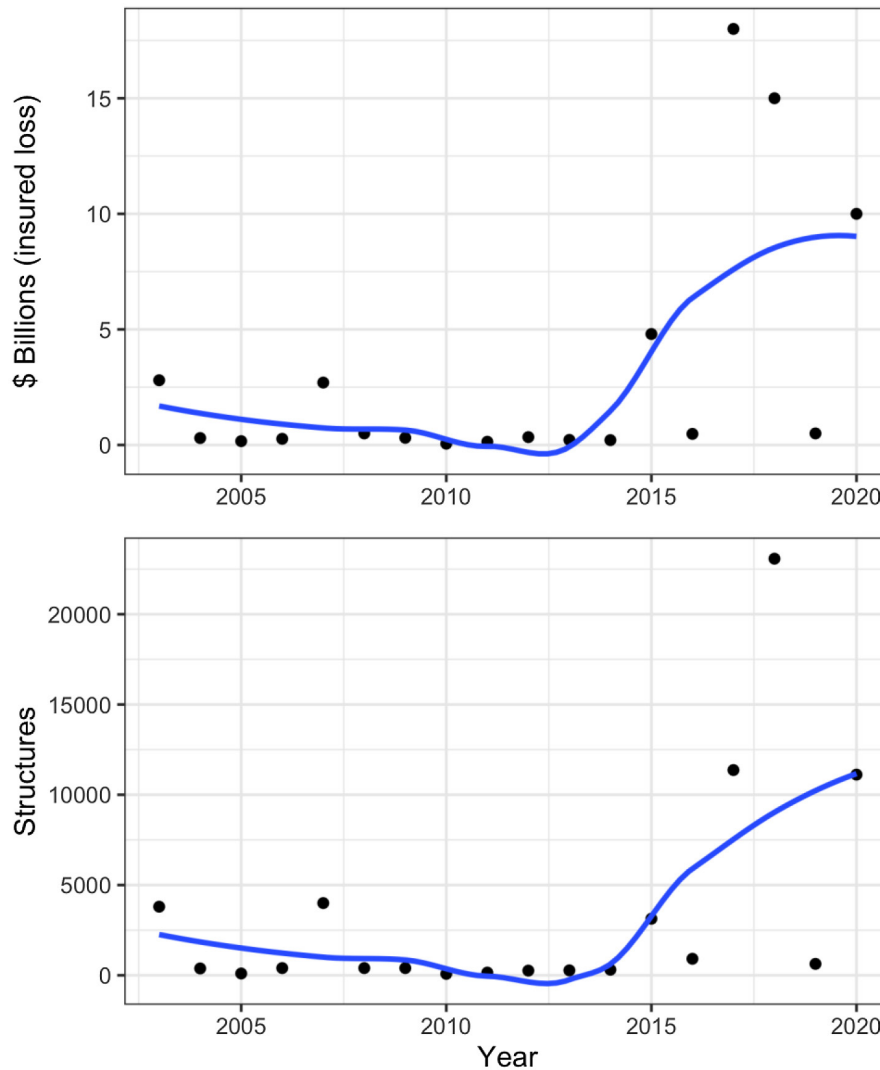


**FIGURE 3** Loess curves fitted to insured economic loss (top panel) and structures destroyed by wildfire (bottom panel) in California, 2003–2020. The first year for which reliable data were available for both variables was 2003. Curves were fitted using a span parameter of 0.75 and second-degree polynomials. Data from: Insurance Information Institute (<https://www.iii.org/fact-statistic/facts-statistics-wildfires>); and Cal Fire annual incident summaries (<https://www.fire.ca.gov/incidents/>)

$p = .011$ ). The long duration of non-wilderness fires was largely attributable to lack of availability of sufficient fire-fighting resources to deal with many high-priority fires at once (CALFIRE, 2020). Similar extreme effects of strained fire-fighting resources on fire response times and delayed containment have occurred in previous big fire years in California, such as 1987 and 2008 (Miller et al., 2012; see Haight & Fried, 2007).

Of the 24 fires >10,000 ha (Table 1), all but two experienced at least one red flag day. For most fires, red flag conditions were coincident with their ignitions, which is not surprising given that meteorological conditions at the time of ignition are a major driver of fire spread and escape from initial attack. The number of red flag days was also correlated with fire duration ( $r = 0.539$ ,  $p = .01$ ), and many of the longer and larger 2020 fires experienced at least one wind-driven reactivation of rapid spread and intense burning many days or weeks after ignition (e.g., the North and August Complexes).

Minimum daily 10-h fuel moistures (FMs) during the first 5 days of burning averaged 3.44% (median = 3.3%,  $SE = 0.143\%$ ), and across the entire duration of the fire, mean daily FMs averaged 5.77% (median = 5.9%,  $SE = 0.253\%$ ) (Table 1). Overall, these are extremely low FMs (S. Stephens, UC-Berkeley, pers. comm.), especially considering that the mean values include nighttime readings. As expected, the lowest FMs were measured in dry desert and interior Coast Range sites (e.g., Dome and Mineral Fires), whereas higher values were measured in montane and coastal sites.

Fire suppression costs in the USA have been skyrocketing (NIFC, 2021). Overall fire suppression costs in California in 2020 approached \$2.1 billion (NIFC, 2020). Based primarily on the NIFC year-end report (NIFC, 2020), the 75 largest fires cost c. \$1.9 billion to extinguish. Overall, the most expensive fires were the biggest (i.e., August Complex, Creek, North Complex and Castle), but the average cost per unit area varied widely. Overall mean cost per

hectare was \$2,454 (median \$1,388,  $SE = \$313$ ), with a maximum of \$12,716 per hectare (Oak Fire, Mendocino County) and a minimum of \$44 per hectare (Rattlesnake Fire, Tulare County, which was managed for resource benefit) (Table 1; Supporting Information Table S1). A comparison of the 10 most costly fires per unit area with the 10 least costly fires per unit area from Table 1 and Supporting Information Table S1 shows that the most costly fires tended to be in or near to heavily or moderately populated areas, were mostly human ignited (8 of 10), resulted in evacuations of hundreds to tens of thousands of people (only the Fork Fire in Eldorado County did not force evacuations), and burned for an average of 30 days. These fires also killed two people, and half of the fires resulted in destroyed structures. The 10 least costly fires per unit area were mostly lightning ignited (6 of 10, with 3 human and 1 unknown), primarily in wilderness (4 fires were resource benefit fires) or rural settings, and burned for an average of c. 59 days. Only two of these fires forced evacuations (Grant, Sacramento County, and Laura 2, Lassen County), and there were no deaths.

The 24 fires >10,000 ha burned a wide variety of vegetation types (Table 2; Supporting Information Table S2). The most commonly burned PFR types were Douglas-fir/mixed evergreen (17.9%), moist mixed conifer (16.6%), chaparral and serotinous conifers (14.7%), and dry mixed conifer (11.2%). Combined, the yellow pine and mixed conifer ("YPMC") types, which are ecologically related (Safford & Stevens, 2017), accounted for 34% of burned area. Conifer-dominated vegetation accounted for 58.3% of burned area, shrub-dominated vegetation contributed 23.8%, hardwood-dominated vegetation (mostly oak) accounted for 9.9%, and undefined types (largely grasslands and meadows, pastures and agricultural lands) totalled 8% (Supporting Information Table S2).

Although the 2020 fires burned through a wide spectrum of previous fire histories, the fires can be split readily into two groups (Supporting Information Table 2): Group 1 (above the horizontal blue line) includes those fires that burned mostly forest-dominated landscapes that had remained largely unburned during the previous 112+ years, whereas Group 2 (below the blue line) includes those fires that burned predominantly previously burned, chaparral-dominated landscapes. All fires in Group 1 are characterized by strongly positive PFRID values, underlining how 100+ years of fire suppression have drastically reduced fire frequencies in Californian conifer forests, especially in the widespread YPMC systems (Safford & Stevens, 2017; Van Wagtenonk et al., 2018). All fires in Group 2, except for the mostly forested Red Salmon, are characterized by low and very low mean PFRID values, underlining the fact that most central and southern Californian chaparral landscapes are being burned more frequently, mostly by human ignitions, than under probable pre-EAS conditions (Safford & Van de Water, 2014).

The extent of prior burning (since 1908) within the 2020 fire perimeters was closely related to vegetation composition. For example, across all fires the percentage of the landscape composed of chaparral and sage scrub was strongly correlated with the percentage of the landscape burned before 2020 ( $r = 0.701$ ,  $p < .001$ ). In California, chaparral and sage scrub habitats tend to burn under two scenarios

(Safford et al., 2018): (1) spring and summer fires generally occur in conditions characterized by relatively higher fuel moistures and moderate onshore winds, conditions in which fuel age/fuel loading plays an important role in limiting burning and fire control actions have success in limiting fire size; and (2) autumn and winter fires that escape initial attack tend to ignite and spread during hot, dry spells influenced by strong offshore föhn winds from the north or east (e.g., the "Santa Ana" winds in southern California), conditions in which fuel age/loading might be nearly irrelevant and fire control is difficult. The 2020 fires provided excellent examples of both scenarios (Figure 4).

Many fires that burned through forested landscapes (Group 1 in Table 2) showed marked spatial limitation by recently burned areas, which are likely to have supported lower fuel loads and/or fuel continuity (e.g., Collins et al., 2009). This was especially the case for areas previously burned  $\leq 10$ –12 years before 2020. The fire return interval in mixed conifer and yellow pine forests in pre-EAS conditions averaged 11–16 years across California (median = 7–12 years; Van de Water & Safford, 2011). Given that these forest types supported a fuel-limited fire regime (Safford & Stevens, 2017; Steel et al., 2015), this frequency should represent roughly the length of time for which fire-driven fuel reduction can resist reburning (at least in historical climate conditions, which were less conducive to burning than today; Parks & Abatzoglou, 2020). In a modern landscape, Collins et al. (2009) found that fuel reduction from wildfires in Yosemite National Park mixed conifer forests persisted for up to c. 9 years after fire, at which point new fires encountered enough fuel to burn in severe fire-weather conditions (high winds and temperatures, low humidities). Both conditions are exemplified by the 2020 fires. The Castle and Slater Fire perimeters were strongly constrained by reduced fuels in recent burns ( $\leq 5$  years old in 2020), and the Red Salmon Fires largely followed the same pattern (constrained by fires  $\leq 7$  years old) but also burned an area of more diverse fire history, including some areas 15, 12 and 7 years old (Figure 5). The North Complex Fire was either constrained or not by a series of 12-year-old fires, depending on weather conditions at the time (Supporting Information Figure S3).

### 3.2 | Fire severity patterns and drivers in 2020

The percentage of area burned at high severity, as measured on our 180-m grid, varied by vegetation type (Figure 6). About 70% of points occupied by sagebrush, chaparral and sage scrub types burned at high severity, and slightly more than half of the montane chaparral (which is generally successional to conifer forest and typically moister and more resistant to burning than lowland chaparral) points burned at high severity (Figure 6). The prevalence of high-severity burning in shrub types is driven by the lack of vertical separation between the ground surface and canopy fuels and by horizontal continuity between shrub canopies (Keeley & Safford, 2016). Postfire recovery is generally rapid (unless sites have been degraded by, e.g., frequent burning, air pollution, invasive grasses) in chaparral and

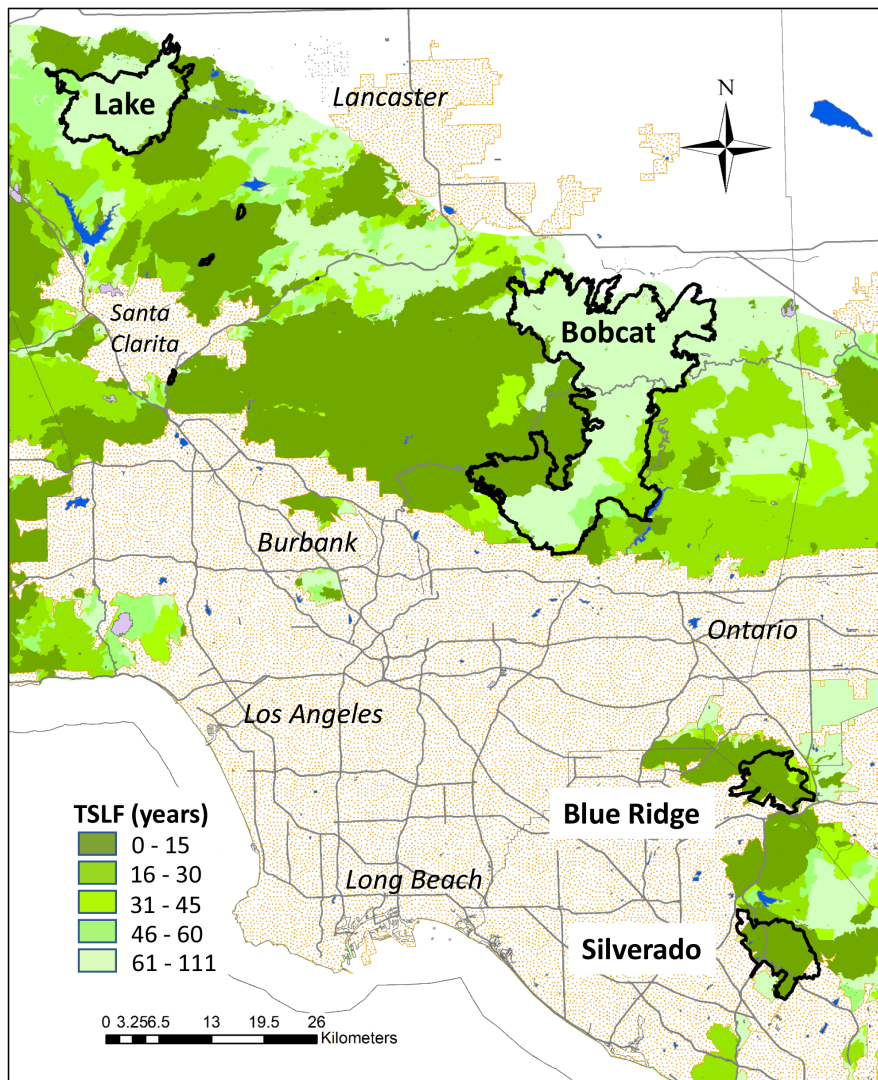


**FIGURE 4** Fire perimeters of four chaparral-dominated 2020 fires in southern California, overlaid on time since last fire (TSLF). The Bobcat and Lake Fires occurred in the summer and were largely fuel limited (except during a few days of high winds) and occurred in areas dominated by TSLF >61 years. The Blue Ridge and Silverado Fires burned during a Santa Ana wind event in the autumn and spread rapidly through younger fuels, in areas with TSLF between 0 and 15 years

sage scrub vegetation, in which the dominant species all resprout and/or generate seeds whose germination is cued by fire (Keeley & Zedler, 1978). On the contrary, most dominant species in the sagebrush types lack resprouting capacity, and fire-cued germination is absent (Sawyer et al., 2009).

In the montane forest types (yellow pine, mixed evergreen, mixed conifer and red fir) the percentage of grid points burned at high severity ranged from 30 to 39% (Figure 6). For the YPMC types, this is three to six times more high-severity burning than in probable pre-EAS reference conditions (Bohlman et al., 2021; Safford & Stevens, 2017). In all montane forest types, burning in 2020 was exceptionally severe in comparison to the average high-severity percentage from the period 1984–2008 (Miller et al., 2009, 2012). In 2020, yellow pine, mixed conifer and red fir forests experienced 43–76% relative increases (12–14% absolute increases) in the area burned at high severity versus the 1984–2008 averages, and mixed evergreen forests in 2020 burned at nearly quadruple the proportion of high severity measured by Miller et al. (2009, 2012) (Figure 6). In these forest types, there are no specific adaptations to high-severity fire among the dominant conifer species (Keeley & Safford, 2016).

Postfire regeneration at a given site depends primarily on the survival of nearby adult trees, which is increasingly impacted by the growing extent of high-severity burning (Shive et al., 2018; Stevens et al., 2017).

We ranked the 38 fires we assessed in our fire severity analyses in descending order with respect to their areal percentage of high-severity burning (Supporting Information Table S3). The highest-severity fires were generally those with extensive areas of shrubland. Total landscape cover of shrublands of all types within the fire perimeter was a strong univariate predictor of high-severity burning ( $r^2 = 0.582$ ,  $p < .001$ ; Supporting Information Figure S4). Fire severity was poorly predicted for a set of wind-driven fires with relatively low shrub cover that experienced higher than expected fire severity (Blue Ridge, North Complex, Sheep, Slater and Zogg; Supporting Information Figure S4). The lowest-severity fires were either in moist forest types that did not experience major wind events (Devil, Red Salmon and Walbridge) or in higher-elevation sites (Bluejay and Rattlesnake, both of which were managed for resource benefit in National Parks) (Supporting Information Table S3).



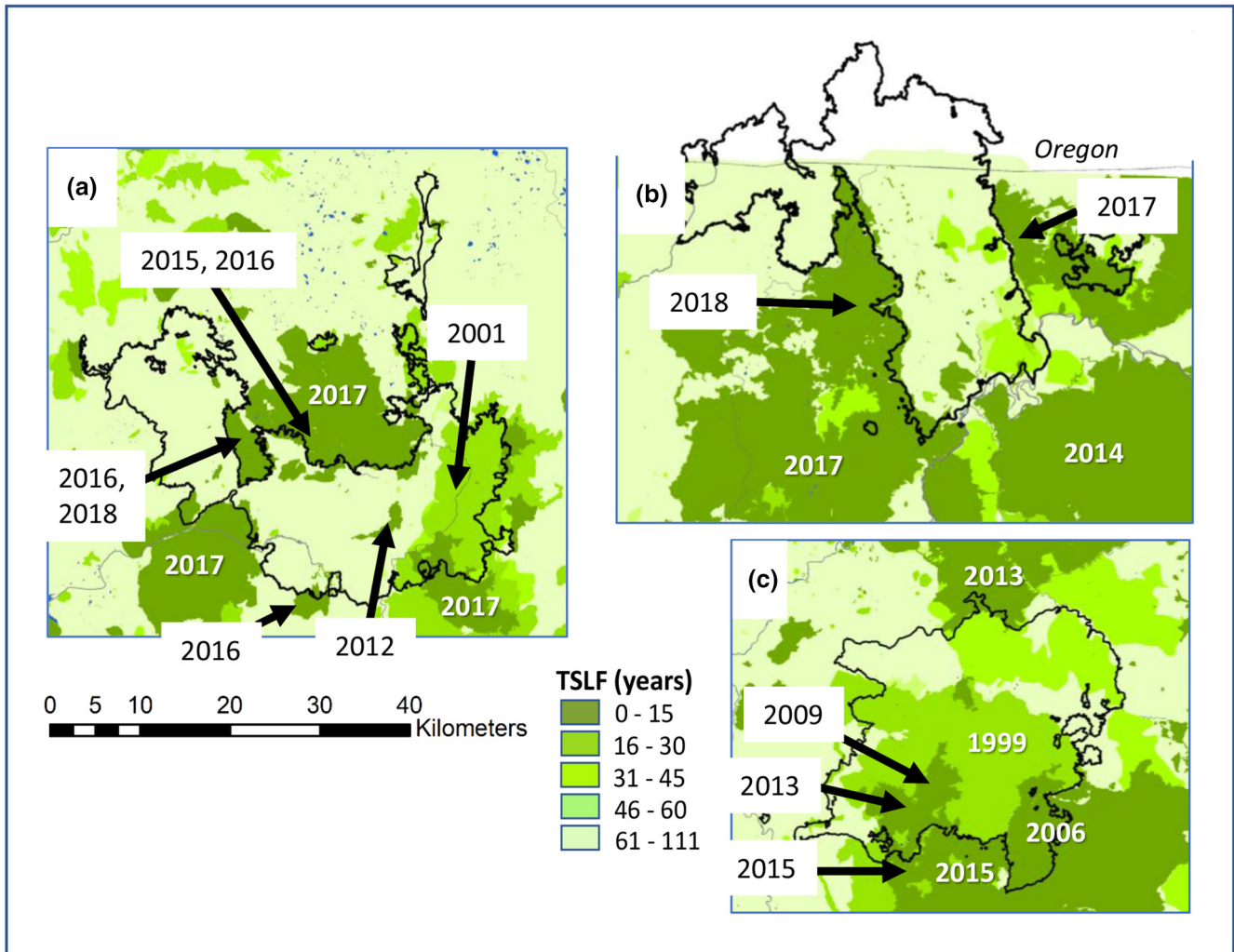
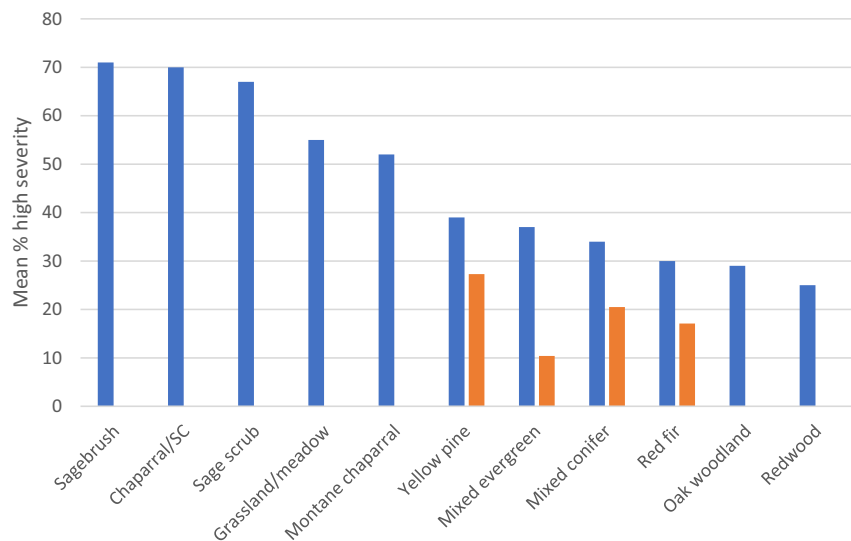


**FIGURE 5** Fire perimeters of three conifer-dominated 2020 fires in northern and central California, overlaid on time since last fire (TSLF). (a) Castle Fire, southern Sierra Nevada. (b) Slater Fire, northern Klamath Mountains (fire return interval departure data lacking north of California–Oregon border). (c) Red Salmon Fire, Klamath Mountains. All subfigures are at the same spatial scale; north is towards the top of the page

**FIGURE 6** Percentage of the 180-m sampling grid that burned at high severity, by vegetation type. Only types with >5,000 points are shown. Values are compared with averaged area-weighted values (orange bars) for four forest types also estimated by Miller et al. (2009, 2012) for the period 1984–2008. “Sagebrush” combines all sagebrush types; “SC” = serotinous conifers; “Mixed conifer” includes both dry and moist mixed conifer



Forest-dominated fires with <20% shrub cover burned at an average of 33.4% high severity.

In our vegetation model for fire severity, VPD and wind speed on the day of burning were positively associated with increasing probability of high-severity fire for all of the vegetation types (Figure 7a,b); all but three vegetation types with >95% probability (Supporting Information Figure S5). TSLF also had a positive

influence on high-severity probability for most of the vegetation types, especially for Douglas-fir/mixed evergreen, YPMC, and chaparral and sage scrub (Figure 7c). Steel et al. (2015) studied the relationship between fire severity and TSLF in Californian forests for the period 1984–2011. They found a similar positive influence of TSLF on the proportion of high-severity fire to the 2020 patterns, but the mean 2020 high-severity values are 1.5–2

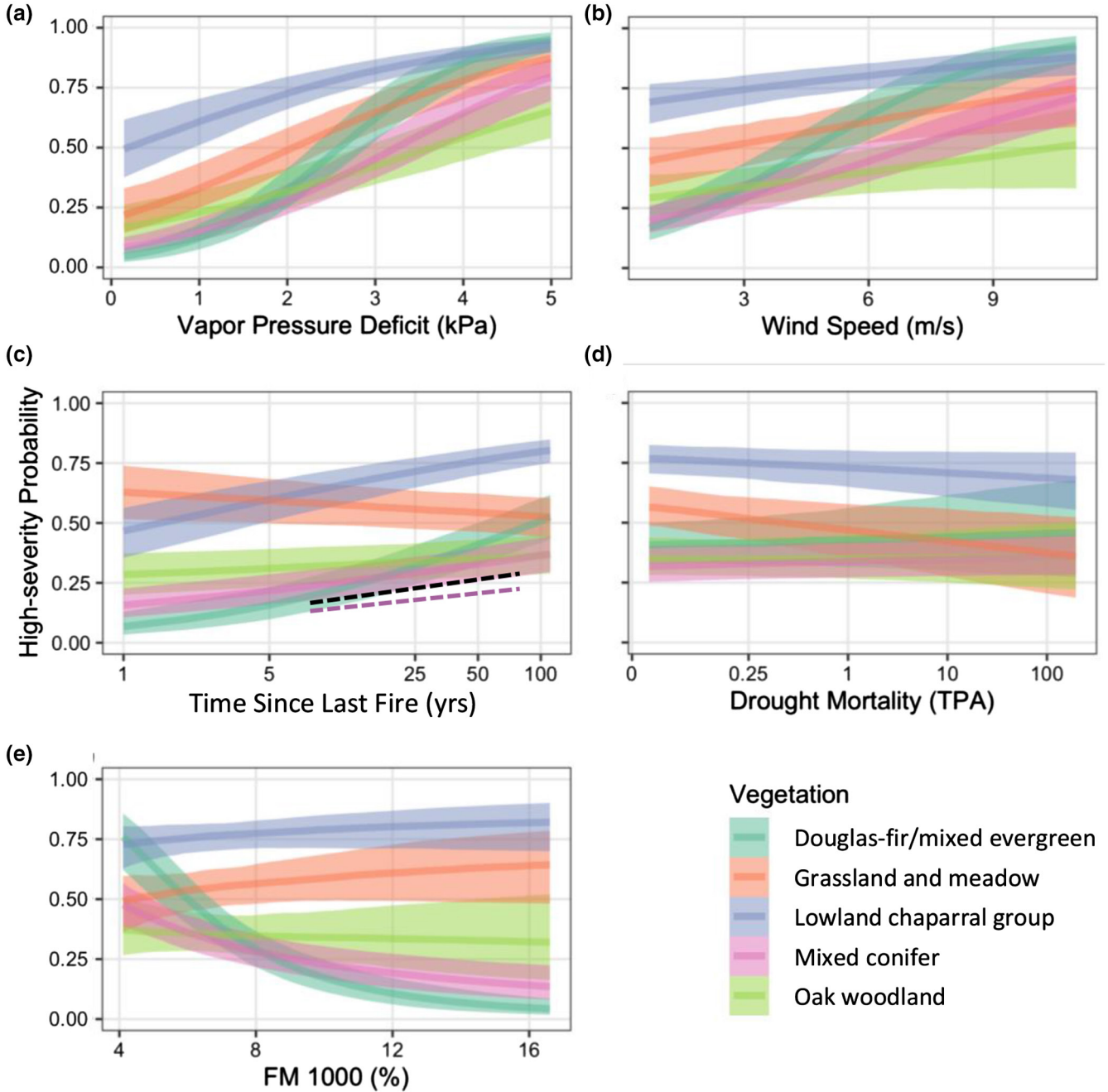


FIGURE 7 Modelled marginal effects of our five predictor variables on the probability of high severity across the thinned 900-m sampling grid for five of the most widely distributed vegetation types. “Lowland chaparral” = chaparral + serotinous conifers + sage scrub. Dashed lines: modelled fire severity × time since last fire prediction for Douglas-fir/mixed evergreen forests (black line) and yellow pine and mixed conifer forests (purple line) for the period 1984–2011, from the study by Steel et al. (2015)



times greater than the 1984–2011 values. As TSLF increased, the proportion of area burned at high severity for the lowland chaparral group increased from 40–55 to 75–80% (Figure 7c). This pattern was probably driven both by increasing live biomass in chaparral stands (W. Oechel, San Diego State University, pers. comm.) and by accumulation of dead fuels owing to the death of short-lived obligate seeders (Keeley & Zedler, 2009). In addition, in 2020 relatively little area in the lowland chaparral group was burned by late season fires in Santa Ana wind conditions, which can overwhelm fuel age/loading limitations. Redwood forest and grassland/meadow were the only vegetation types where the high-severity probability exhibited a credible negative relationship to TSLF (Figure 7c; Supporting Information Figure S5). This might stem from the fact that areas in these types that have escaped burning the longest might be the most fire resistant (e.g., maritime climate influence or moist edaphic microsites, both common for these vegetation types).

Drought mortality was related to increased probability of high-severity fire with high model confidence ( $\geq 95\%$  probability) in the white fir (part of the mixed conifer PFR) and montane hardwood (mixed evergreen PFR) CWHR types, and with moderate model confidence ( $\geq 90\%$  probability) for yellow pine, mixed conifer and red fir (Figure 7d; Supporting Information Figure S5). Chaparral types (montane and lowland) and grassland showed negative relationships between drought mortality (which was measured in trees) and high-severity probability (Supporting Information Figure S5). Modelled 1,000-h fuel moisture, which represents more long-term effects of seasonal or annual aridity (assuming large-diameter woody fuels are present), showed a strong inverse relationship with high-severity probability in Douglas-fir/mixed evergreen and mixed conifer forests, especially below 8–10% fuel moisture, but showed little importance for other vegetation types, particularly chaparral, grassland and oak woodland, where 1,000-h fuels are usually absent or only a minor component of the fuel load (Figure 7e). Overall, the probability of high-severity burning in our vegetation-based model was influenced primarily by a combination of short-term meteorological conditions (VPD and wind) and TSLF, which is a surrogate for fuel accumulation (very little of the state has experienced fuel reduction not accomplished by wildland fire), with contributions from longer-term drought-related variables, such as 1,000-h fuel moisture and tree mortality, in some of the montane forest types.

Our fire model estimated credibly positive effects of VPD, wind speed and TSLF on burn severity and uncertain effects of 1,000-h fuels and drought mortality at the population level (i.e., among all fires; Supporting Information Table S4). However, the strength of these effects varied greatly among individual fires (Table 3; Supporting Information Figure S6). Table 3 compares median odds ratios for the occurrence of high-severity fire across our 900-m sampling grid for 38 large fires from 2020. Odds ratios are relative to the 2020 sample, where values above one represent greater than average likelihood of high-severity effects given

the conditions of an individual fire and those below one represent below average likelihood of high severity. For 10 fires, high-severity effects were credibly more likely than average given the TSLF of a fire [95% odds ratio credible/confidence interval (CI) did not include one], with an 11th also likely to be above the 2020 mean (90% CI did not include one; Table 3). For example, high-severity fire was 55% more likely (odds ratio of 1.55) in the Slater Fire than the 2020 mean owing to its TSLF condition. Fires that burned large areas of previously unburned (since 1908) forest were especially prone to expansive high-severity burning. Three of these (Castle, Slater and North Complex) are shown in Figure 5 and Supporting Information Figure S2. CZU and Hennessey showed credibly lower likelihood of high-severity fire attributable to TSLF than average. High-severity burning in CZU was wind driven (but in older fuels), and Hennessey burned a highly human-altered region, where almost 40% of the landscape had burned in the previous 10 years (Table 2).

The two meteorological variables were also important drivers of high-severity fire occurrence. Vapour pressure deficit was a highly credible driver of high-severity effects in seven fires and wind speed in six (Table 3). The fires with strong effects of VPD on high-severity burning were found almost entirely at low to middle elevations in the Coast Ranges or southern California (Bobcat, Glass, Hennessey and SCU) or in other parts of the state characterized by hot, dry conditions in mid-summer (North Complex and Loyaltan); the Slater Fire is the anomaly in this group. Shrub, grassland and agricultural landscapes were also characteristic of many of these fires (Table 2; Supporting Information Table S3). Wind speed had a monumental impact on burning on the CZU Complex (high severity was 159 times more likely than average), such that essentially all high-severity pixels were burned on a handful of very windy days (Table 3).

Although 1,000-h fuel moisture was not a consistently important driver of high severity across fires, three lightning complex fires showed a highly credible effect of this variable: the North Complex, SCU and August (Table 3; Supporting Information Figure S6). All three fires began in mid-August and burned in northern and central Californian regions that were in severe drought conditions by the second half of August (US Drought Monitor; <https://droughtmonitor.unl.edu>).

Drought mortality effects on high-severity occurrence were mostly weak and credible intervals very wide. The only fire with a highly credible effect of drought mortality was the Castle Fire, with the Creek Fire showing a moderately credible effect (Table 3). This was not surprising, because the Castle and Creek Fires were the only large fires to burn in areas heavily impacted by tree mortality stemming from the 2012–2016 drought (Young et al., 2017).

To summarize: fuels and weather variables both make important contributions to high-severity fire, but their relative contributions vary notably among vegetation types and fires; 2020 gives us some specific examples of when severity was predominantly driven by fuels (e.g., Apple and Mineral Fires, in addition to Castle

**TABLE 3** Odds ratios for five predictor variables and their influence on the occurrence of high-severity fire, from statistical model fitted to the 900-m point grid

Fire	TSLF	VPD	Wind speed	1,000-h fuel moisture	Drought mortality	Number of highly credible factors
Apple	1.109	1.062	0.938	0.998	0.96	1
August Complex	1.217	0.86	0.869	1.028	1.019	4
Blue Ridge	0.779	0.902	1.02	1.81	0.996	0
Bluejay	0.962	0.728	0.889	1.003	1.047	0
Bobcat	0.975	1.037	0.978	0.462	1.009	2
Caldwell	1.157	1.054	0.93	0.178	0.999	2
Carmel	1.088	0.936	4.892	0.682	1.015	0
Castle	1.344	0.875	0.721	0.406	1.314	5
Creek	1.108	0.512	0.974	0.662	1.208	4
CZU	0.677	0.991	158.845	0.893	1.162	2
Devil	0.71	0.672	0.735	1.081	1.016	0
Dolan	0.878	0.951	1.135	0.985	1.015	2
Glass	1.223	2.195	0.964	0.959	1.018	2
Gold	1.088	1.024	0.747	1.004	1.021	0
Hennessey	0.822	1.944	1.084	0.818	1.035	4
Hog	1.13	1.075	0.923	1.016	0.997	0
Lake	1.182	2.09	0.805	1.096	0.99	0
Loyalton	1.403	1.031	0.966	1.005	0.941	2
Mineral	1.304	1.26	0.861	1.006	1.009	2
North	1.194	1.078	0.911	1.021	0.987	0
North Complex	1.168	1.082	1.702	1.991	0.983	4
Rattlesnake	1.319	0.268	0.56	1.795	0.964	1
Red Salmon	0.982	0.826	0.899	0.709	1.045	3
River	1.026	1.001	1.001	1.26	1.045	0
SCU	1.117	1.166	1.116	1.025	1.045	3
Sheep	1.036	0.679	1.368	0.986	0.989	2
Silverado	0.823	0.677	1.052	2.542	1.003	0
Slater	1.551	1.582	1.157	0.98	0.912	4
Slink	0.794	1.804	0.998	0.991	1.11	0
Snow	0.976	1.049	1.309	0.243	1.035	0
Stagecoach	1.089	0.968	1.217	1.03	0.954	0
Valley	0.987	2.097	1.081	0.719	1.008	0
W-5 Cold Springs	1.217	0.737	0.978	1.728	0.948	1
Walbridge	1.073	0.666	1.613	0.612	1.052	1
Zogg	1.111	1.1	0.609	1.123	0.978	1

Note: Odds ratios are relative to the expected value for the 2020 fires assessed, where values greater than one represent greater than average effects of a given predictor and those less than one represent below average effects. Odds ratios are listed side by side for each of the five predictor variables. Values in the orange cells represent effects that are credibly higher than one (which represents the mean across all pixels in all fires for each variable) at a credibility/confidence interval (CI) of 95% (we call these "highly credible"). Bold values in these cells identify the most important credible driver of fire severity for the fire indicated. Yellow cells represent effects that are credibly higher than one with a CI of 90% (we call these "moderately credible"). Green cells pertain to effects that were less [with high credibility (CI 95%)] than the average across all fires, and blue cells represent effects that were less than the average with moderate credibility (CI 90%).

Abbreviations: TSLF, time (in years) since last fire; VPD, vapour pressure deficit.

and Creek Fires with an important contribution of prefire drought mortality) versus predominantly driven by weather (e.g., CZU, Hennessey and Dolan Fires), but many fires showed a combination

of fuels, weather and other variables that was contingent on spatial and temporal variation in the burn environment (e.g., Slater, North and SCU Fires).

### 3.3 | Conclusions

Although the 2020 fire season was an eye-opener for human participants and observers, it continued a trend of progressively more extensive and severe burning that has been ongoing for the last 20 years or more. The unexpected occurrence of a 3-day lightning storm along the coast in the usually dry heat of August and the magnitude of the jump in burned area between 2019 and 2020 (>16 times) were perhaps the most surprising phenomena, but the subsequent extent of burning in 2021 (which would have been the record year if it were not for the August 2020 lightning outbreak) underlines that 2020 was not a fluke. Nothing we've seen suggests that current trends will abate, and all credible models of projected future fire activity, area and behaviour agree that: (1) California is in for a very smoky future, and (2) the continued resilience and even persistence of numerous terrestrial ecosystems is not assured (Restaino & Safford, 2018; Safford et al., 2012; Serra-Diaz et al., 2018). In addition, socio-economic impacts and the underappreciated effects of large-scale severe burning on human health will continue to accrue.

Taking the long view, 2020 was the first fire year since records have been available (first half of the 20th century) when burned area has come anywhere close to pre-EAS estimates. Considering current trends, it seems reasonable to wonder whether we are seeing a long-overdue rebound to more normal levels of burning after a century of spectacular "success" in erasing fire as an ecological force in much of the state. The problem is that much of the burning we are seeing is not restorative but destructive (Mallek et al., 2013; Safford et al., 2021). Fuel reduction on large landscapes will be necessary in order to realize the ecological and fire-safety benefits of the inevitably broader extents of burning that will occur in Californian forests in coming years. Management agency focus continues to be on active fuel management (mechanical and hand thinning), but this is severely limited by agency budgets and capacity, the lack of sawmills and other economic outlets, and the fact that only 30–40% of the Forest Service land base (and much less of the National Park land base) in California is even treatable owing to logistical, jurisdictional and topogeographical constraints (North et al., 2012). Interest in prescribed fire has experienced a major increase in California, with agencies, tribes and private citizens all expanding their training, planning and implementation activities (Safford et al., 2021), but even tripling or quadrupling the area of prescribed burning in California would constitute a drop in the bucket compared with the need (North et al., 2012). The importance of recent fire history in influencing fire spread and fire severity underlines the key role that wildfire can and must play in reducing fuels on large landscapes. Like it or not, the vast bulk of burning that occurs in California will always occur in areas that have not experienced active fuel reduction activities. Assuming constant fuels, the most severe burning occurs during periods of extreme fire-weather, which occur on only 5–10% of the days. This leaves much of the fire season (with the size of the window admittedly shrinking as the climate warms) available for management of wildfires for resource benefits and fuel reduction. Successful managed wildfire programmes in the Californian national

parks have always been a beacon for fire use across the state (van Wagtenonk & Lutz, 2007). Recently, the Forest Service has used advanced fire risk assessments (Thompson et al., 2016) to designate large areas in recent land and resource management plans (LRMPs) in the southern Sierra Nevada as fire maintenance or fire restoration zones, where naturally ignited fires will be permitted to burn in appropriate weather conditions (USDA, 2019). Additionally, the national forests in north-western California are in the initial stages of LRMP revision, and a fire risk assessment for that region is getting underway.

Much more concerning than the area of burning during the 2020 fire season was the exceptional severity of burning that forest ecosystems experienced. The proportion of high-severity burning in montane forests in 2020 averaged 43–76% higher than the 25-year average between 1984 and 2008 and was three to six times higher than under pre-EAS reference conditions (2021 was also a year of very severe burning). In these forest types, such severe burning can have major ecosystem consequences, including increased soil erosion and stream sedimentation, enduring impacts on biogeochemical cycles, massive emissions and carbon loss, and negative effects on many biota (CALFIRE, 2020; Dove et al., 2020; Jones et al., 2021; Safford et al., 2021; Scott et al., 2009; State of California, 2018). In addition, postfire regeneration of the dominant conifers (none of which is serotinous) in these ecosystems is greatly hampered by the loss of adult trees over large areas. Welch et al. (2016) found that areas of montane forest experiencing  $\geq 75\%$  fire-caused mortality did not generally support seedling densities that met Forest Service stocking guidelines, and in areas experiencing  $\geq 90\%$  mortality the median seedling density 5 years post-fire was zero. The area of high-severity burning ( $\geq 95\%$  basal area mortality in our definition) in 2020 in Californian montane forests approached 300,000 ha, with hundreds of thousands more hectares between 75 and 95% mortality. Replanting will be necessary to restore conifer forests in much of this area, but the need for replanting is orders of magnitude greater than the current maximum production capacity of combined Forest Service and CALFIRE nursery and planting programmes in California (J. Sherlock, US Forest Service, pers. comm.). Postfire competition with shrubs, the warming climate and the potential for short-interval reburning are all major impediments to success in restoring conifer forests in California (Coppoletta et al., 2016; Safford & Vallejo, 2019; Steel et al., 2021; Stewart et al., 2021; Tepley et al., 2017), and dealing with them will require new ways of doing business. These include reducing planting densities, planting a greater variety of seedling genotypes, better tailoring of planting to local microenvironments, replacing conifers with native broadleaf species in some areas, and developing alternatives to the standard timber-production focus of reforestation (North et al., 2019).

Five decades ago, the US federal land and resource management agencies made a much-acclaimed transition from full fire suppression to "ecological fire management" (Stephens & Ruth, 2005), yet today the gulf between fire operations and resource management in the agencies is arguably as wide as it has ever been.

Agency success in managing fire is still gauged as a function of reducing the area burned, although we have known for half a century or more that the artificial reduction of burned area in frequent-fire forests leads inexorably to stand densification and fuel accumulation (Safford et al., 2021; Steel et al., 2015). Thirty years after the move to ecological fire management, the 2000 National Fire Plan redirected federal agencies to emphasize human asset protection (Botti & Nichols, 2021). In the years since, steady erosion has occurred in the resource management capacities of federal and many state agencies, such that fire operations budgets have ballooned (with little apparent effect on national wildfire trends), but fuel reduction, fire prevention and reforestation/restoration budgets have dwindled. Today, we find ourselves in a “firefighting trap”, where our short-term “successes” are leading to long-term losses, as fires grow in intensity and size beyond our ability to stop them, and the environment and its human beneficiaries pay the price (Moreira et al., 2020; North et al., 2015). In ecosystems such as these, focus should not be on reducing burned area (indeed, the opposite is true) but rather on reducing the severity of burning when it occurs and on restoring key ecosystem functions where severe burning has transpired. Recent developments in California, including the signing of a memorandum of understanding between the State and the Forest Service, which seeks to increase fuel reduction activities greatly, and the recent California Wildfire and Forest Resilience Action Plan (Safford et al., 2021; State of California, 2021) suggest that the message is finally getting through, but there is no time to lose.

## ACKNOWLEDGMENTS

Thanks to Chad Roberts and Daniel Matthews for constructive reviews of the draft manuscript.

## CONFLICT OF INTEREST

We declare no conflicts of interest.

## AUTHOR CONTRIBUTIONS

H.D.S. conceived the study, collected and analysed data and wrote the paper. A.K.P., Z.L.S., D.J.N.Y. and R.B.W. collected and analysed data and wrote the paper.

## DATA AVAILABILITY STATEMENT

Most of the data analysed in this study are publicly available, and links are provided in the paper and in the Supporting Information. The derivative data used in the assessment of fire severity patterns are archived at OSF (<https://osf.io/8mw9e/settings/>), and the code used to complete the fire severity analyses is available at: [https://github.com/akpaulson/2020\\_Fires\\_GEB](https://github.com/akpaulson/2020_Fires_GEB)

## ORCID

Hugh D. Safford  <https://orcid.org/0000-0002-0608-6728>

Alison K. Paulson  <https://orcid.org/0000-0003-2068-3999>

Derek J. N. Young  <https://orcid.org/0000-0003-2465-0254>

## REFERENCES

- Abatzoglou, J. T. (2013). Development of gridded surface meteorological data for ecological applications and modelling. *International Journal of Climatology*, 33, 121–131. <https://doi.org/10.1002/joc.3413>
- Agee, J. K. (1993). *Fire ecology of Pacific Northwest forests*. Island Press.
- Aguilera, R., Corringham, T., Gershunov, A., & Benmarhnia, T. (2021). Wildfire smoke impacts respiratory health more than fine particles from other sources: Observational evidence from Southern California. *Nature Communications*, 12(1), 1–8. <https://doi.org/10.1038/s41467-021-21708-0>
- Aon. (2021). 2020 weather, climate and catastrophe report. <https://www.aon.com/global-weather-catastrophe-natural-disasters-costs-climate-change-2020-annual-report/index.html>
- Bailey, R. G. (1995). Descriptions of the ecoregions of the United States (2nd ed.). Misc. Publ. 1391. USDA Forest Service.
- Bohlman, G., Skinner, C., & Safford, H. D. (2021). Natural range of variation (NRV) for yellow pine and mixed conifer forests in northwestern California and southwestern Oregon. General Technical Report PSW-GTR-273, USDA Forest Service, Pacific Southwest Research Station, Albany, CA.
- Botti, S., & Nichols, T. (2021). National Park Service fire restoration, policies versus results: What went wrong. *Parks Stewardship Forum*, 37(2), 353–367. <https://doi.org/10.5070/P537253241>
- Bürkner, P.-C. (2017). brms: An R package for Bayesian multilevel models using Stan. *Journal of Statistical Software*, 80, 1–28.
- CALFIRE. (2020). 2020 fire siege. California Department of Fire and Forest Protection, Sacramento, CA. [www.fire.ca.gov](http://www.fire.ca.gov)
- Cleland, S. E., West, J. J., Jia, Y., Reid, S., Raffuse, S., O'Neill, S., & Serre, M. L. (2020). Estimating wildfire smoke concentrations during the October 2017 California fires through BME space/time data fusion of observed, modeled, and satellite-derived PM<sub>2.5</sub>. *Environmental Science & Technology*, 54(21), 13439–13447.
- Collins, B. M., Miller, J. D., Thode, A. E., Kelly, M., Van Wagtenonk, J. W., & Stephens, S. L. (2009). Interactions among wildland fires in a long-established Sierra Nevada natural fire area. *Ecosystems*, 12, 114–128. <https://doi.org/10.1007/s10021-008-9211-7>
- Coppoletta, M., Merriam, K. E., & Collins, B. M. (2016). Post-fire vegetation and fuel development influences fire severity patterns in reburns. *Ecological Applications*, 26, 686–699. <https://doi.org/10.1890/15-0225>
- Deryugina, T., Heutel, G., Miller, N. H., Molitor, D., & Reif, J. (2019). The mortality and medical costs of air pollution: Evidence from changes in wind direction. *American Economic Review*, 109, 4178–4219. <https://doi.org/10.1257/aer.20180279>
- Dove, N. C., Safford, H. D., Bohlman, G. N., Estes, B. E., & Hart, S. C. (2020). High-severity wildfire leads to multi-decadal impacts on soil biogeochemistry in mixed conifer forests. *Ecological Applications*, 30, e02072. <https://doi.org/10.1002/eap.2072>
- Haight, R. G., & Fried, J. S. (2007). Deploying wildland fire suppression resources with a scenario-based standard response model. *INFOR: Information Systems and Operational Research*, 45, 31–39. <https://doi.org/10.3138/infor.45.1.31>
- Higuera, P. E., & Abatzoglou, J. T. (2020). Record-setting climate enabled the extraordinary 2020 fire season in the western United States. *Global Change Biology*, 27, 1–2.
- Jones, G. M., Keyser, A. R., Westerling, A. L., Baldwin, W. J., Keane, J. J., Sawyer, S. C., Clare, J. D. J., Gutiérrez, R. J., & Peery, M. Z. (2021). Forest restoration limits megafires and supports species conservation under climate change. *Frontiers in Ecology and the Environment*. <https://doi.org/10.1002/fee.2450>
- Kane, V. R., Cansler, C. A., Povak, N. A., Kane, J. T., McGaughey, R. J., Lutz, J. A., Churchill, D. J., & North, M. P. (2015). Mixed severity fire effects within the Rim fire: Relative importance of local climate, fire weather, topography, and forest structure. *Forest*

- Ecology and Management*, 358, 62–79. <https://doi.org/10.1016/j.foreco.2015.09.001>
- Keeley, J. E., & Safford, H. D. (2016). Fire as an ecosystem process. In H. A. Mooney, & E. Zavaleta (Eds.), *Ecosystems of California* (pp. 27–45). University of California Press.
- Keeley, J. E., Safford, H. D., Fotheringham, C. J., Franklin, J., & Moritz, M. A. (2009). The 2007 Southern California wildfires: Lessons in complexity. *Journal of Forestry*, 107, 287–296.
- Keeley, J. E., & Syphard, A. D. (2021). Large California wildfires: 2020 fires in historical context. *Fire Ecology*, 17(1), 1–11. <https://doi.org/10.1186/s42408-021-00110-7>
- Keeley, J. E., & Zedler, P. H. (1978). Reproduction of chaparral shrubs after fire: A comparison of sprouting and seeding strategies. *American Midland Naturalist*, 99(1), 142–161. <https://doi.org/10.2307/2424939>
- Keeley, J. E., & Zedler, P. H. (2009). Large, high-intensity fire events in southern California shrublands: Debunking the fine-grain age patch model. *Ecological Applications*, 19, 69–94. <https://doi.org/10.1890/08-0281.1>
- Key, C. H., & Benson, N. C. (2006). Landscape assessment: ground measure of severity, the composite burn index. In D. C. Lutes (Ed.), *FIREMON: Fire effects monitoring and inventory system* (pp. LA8–LA15). USDA Forest Service Technical Report RMRS-GTR-164-CD, Rocky Mountain Research Station.
- Kolden, C. (2020). Wildfires: Count lives and homes, not hectares burnt. *Nature*, 586, 9. <https://doi.org/10.1038/d41586-020-02740-4>
- Littell, J. S., McKenzie, D., Peterson, D. L., & Westerling, A. L. (2009). Climate and wildfire area burned in western US ecoprovinces, 1916–2003. *Ecological Applications*, 19, 1003–1021. <https://doi.org/10.1890/07-1183.1>
- Lydersen, J. M., Collins, B. M., Miller, J. D., Fry, D. L., & Stephens, S. L. (2016). Relating fire-caused change in forest structure to remotely sensed estimates of fire severity. *Fire Ecology*, 12, 99–116. <https://doi.org/10.4996/fireecology.1203099>
- Mallek, C. R., Safford, H. D., Viers, J. H., & Miller, J. D. (2013). Modern departures in fire severity and area vary by forest type, Sierra Nevada and southern Cascades, California, USA. *Ecosphere*, 4(12), art153. <https://doi.org/10.1890/ES13-00217.1>
- Marlon, J. R., Bartlein, P. J., Gavin, D. G., Long, C. J., Anderson, R. S., Briles, C. E., Brown, K. J., Colombaroli, D., Hallett, D. J., Power, M. J., Scharf, E. A., & Walsh, M. K. (2012). Long-term perspective on wildfires in the western USA. *Proceedings of the National Academy of Sciences of United States of America*, 109, E535–E543. <https://doi.org/10.1073/pnas.1112839109>
- McClure, C. D., & Jaffe, D. A. (2018). US particulate matter air quality improves except in wildfire-prone areas. *Proceedings of the National Academy of Sciences of United States of America*, 115, 7901–7906. <https://doi.org/10.1073/pnas.1804353115>
- Miller, J. D., & Quayle, B. (2015). Calibration and validation of immediate post-fire satellite-derived data to three severity metrics. *Fire Ecology*, 11, 12–30. <https://doi.org/10.4996/fireecology.1102012>
- Miller, J. D., Safford, H. D., Crimmins, M., & Thode, A. E. (2009). Quantitative evidence for increasing forest fire severity in the Sierra Nevada and southern Cascade Mountains, California and Nevada, USA. *Ecosystems*, 12, 16–32. <https://doi.org/10.1007/s10021-008-9201-9>
- Miller, J. D., Safford, H. D., & Welch, K. R. (2016). Using one year post-fire severity assessments to estimate longer-term effects of fire in conifer forests of northern and eastern California, USA. *Forest Ecology and Management*, 382, 168–183.
- Miller, J. D., Skinner, C. N., Safford, H. D., Knapp, E. E., & Ramirez, C. M. (2012). Trends and causes of severity, size, and number of fires in northwestern California, USA. *Ecological Applications*, 22, 184–203. <https://doi.org/10.1890/10-2108.1>
- Miller, J. D., & Thode, A. E. (2007). Quantifying burn severity in a heterogeneous landscape with a relative version of the delta Normalized Burn Ratio (dNBR). *Remote Sensing of Environment*, 109, 66–80. <https://doi.org/10.1016/j.rse.2006.12.006>
- Moreira, F., Ascoli, D., Safford, H., Adams, M. A., Moreno, J. M., Pereira, J. M. C., Catry, F. X., Armeto, J., Bond, W., González, M. E., Curt, T., Koutsias, N., McCaw, L., Price, O., Pausas, J. G., Rigolot, E., Stephens, S., Tavsanoglu, C., Vallejo, V. R., ... Fernandes, P. M. (2020). Wildfire management in Mediterranean-type regions: Paradigm change needed. *Environmental Research Letters*, 15, 011001. <https://doi.org/10.1088/1748-9326/ab541e>
- Navarro, K., & Vaidyanathan, A. (2020). Notes from the field: Understanding smoke exposure in communities and fire camps affected by wildfires—California and Oregon, 2020. *Morbidity and Mortality Weekly Report*, 69(49), 1873.
- NIFC. (2020). National large incident year-to-date report, Dec. 21, 2020. National Interagency Fire Center. <https://gacc.nifc.gov/sacc/predictive/intelligence/NationalLargeIncidentYTDReport.pdf>
- NIFC. (2021). Federal firefighting costs. 1985–2020. National Interagency Fire Center. <https://www.nifc.gov/fire-information/statistics/suppression-costs>
- North, M., Collins, B. M., & Stephens, S. L. (2012). Using fire to increase the scale, benefits, and future maintenance of fuels treatments. *Journal of Forestry*, 110, 392–401. <https://doi.org/10.5849/jof.12-021>
- North, M. P., Stephens, S. L., Collins, B. M., Agee, J. K., Aplet, G., Franklin, J. F., & Fule, P. Z. (2015). Reform forest fire management. *Science*, 349, 1280–1281. <https://doi.org/10.1126/science.aab2356>
- North, M. P., Stevens, J. T., Greene, D. F., Coppoletta, M., Knapp, E. E., Latimer, A. M., Restaino, C. M., Tompkins, R. E., Welch, K. R., York, R. A., Young, D. J. N., Axelson, J. N., Buckley, T. N., Estes, B. L., Hager, R. N., Long, J. W., Meyer, M. D., Ostoja, S. M., Safford, H. D., ... Wyrsh, P. (2019). Tamm review: Reforestation for resilience in dry western U.S. forests. *Forest Ecology and Management*, 432, 209–224. <https://doi.org/10.1016/j.foreco.2018.09.007>
- Noss, R. F., Franklin, J. F., Baker, W. L., Schoennagel, T., & Moyle, P. B. (2006). Managing fire-prone forests in the western United States. *Frontiers in Ecology and the Environment*, 4, 481–487.
- Parks, S. A. (2014). Mapping day-of-burning with coarse-resolution satellite fire-detection data. *International Journal of Wildland Fire*, 23, 215–223. <https://doi.org/10.1071/WF13138>
- Parks, S. A., & Abatzoglou, J. T. (2020). Warmer and drier fire seasons contribute to increases in area burned at high severity in western US forests from 1985 to 2017. *Geophysical Research Letters*, 47(22), p.e2020GL089858. <https://doi.org/10.1029/2020GL089858>
- Parks, S. A., Holsinger, L. M., Voss, M. A., Loehman, R., & Robinson, N. P. (2018). Mean composite fire severity metrics computed with Google Earth Engine offer improved accuracy and expanded mapping potential. *Remote Sensing*, 10, 879. <https://doi.org/10.3390/rs10060879>
- R Core Team (2020). *R: A language and environment for statistical computing*. R Foundation for Statistical Computing.
- Restaino, C. R., & Safford, H. D. (2018). Fire and climate change. In J. Van Wagtenonk, N. G. Sugihara, S. L. Stephens, A. E. Thode, K. E. Shaffer, & J. Fites-Kaufman (Eds.), *Fire in California's ecosystems* (2nd ed., pp. 493–505). University of California Press.
- Safford, H. D., Butz, R. J., Bohlman, G. N., Coppoletta, M., Estes, B. L., Gross, S. E., Merriam, K. E., & Wuenschel, A. (2021). Fire ecology of the North American Mediterranean-climate zone. chapter 7. In B. Collins, & C. H. Greenberg (Eds.), *Fire ecology and management: Past, present, and future of US forested ecosystems*. Springer.
- Safford, H. D., North, M. P., & Meyer, M. D. (2012). Climate change and the relevance of historical forest conditions. In M. P. North (Ed.), *Managing Sierra Nevada forests* (pp. 23–46). General Technical Report PSW-GTR-237. USDA Forest Service Pacific Southwest Research Station.



- Safford, H. D., & Stevens, J. T. (2017). *Natural Range of Variation (NRV) for yellow pine and mixed conifer forests in the Sierra Nevada, southern Cascades, and Modoc and Inyo National Forests, California, USA*. General Technical Report PSW-GTR-256. USDA Forest Service, Pacific Southwest Research Station
- Safford, H. D., Underwood, E. C., & Molinari, N. A. (2018). Managing chaparral resources on public lands. In E. C. Underwood, H. D. Safford, N. A. Molinari, & J. E. Keeley (Eds.), *Valuing chaparral: Ecological, socioeconomic, and management perspectives* (pp. 411–448). Springer.
- Safford, H. D., & Vallejo, V. R. (2019). Ecosystem management and ecological restoration in the anthropocene: Integrating global change, soils, and disturbance in boreal and mediterranean forests. In M. Busse, D. Dumroese, C. Giardina, & D. Morris (Eds.), *Global change and forest soils: Conservation of a finite natural resource* (pp. 259–308). Elsevier.
- Safford, H. D., & Van de Water, K. M. (2014). *Using Fire Return Interval Departure (FRID) analysis to map spatial and temporal changes in fire frequency on National Forest lands in California*. Research Paper PSW-RP-266. USDA Forest Service, Pacific Southwest Research Station.
- Sawyer, J. O., Keeler-Wolf, T., & Evens, J. M. (2009). *Manual of California vegetation*. California Native Plant Society.
- Scott, D. F., Curran, M. P., Robichaud, P. R., & Wagenbrenner, J. W. (2009). Soil erosion after forest fire. In A. Cerdá, & P. R. Robichaud (Eds.), *Fire effects on soils and restoration strategies* (pp. 193–212). CRC Press.
- Serra-Diaz, J. M., Maxwell, C., Lucash, M. S., Scheller, R. M., Laflower, D. M., Miller, A. D., Tepley, A. J., Epstein, H. E., Anderson-Teixeira, K. J., & Thompson, J. R. (2018). Disequilibrium of fire-prone forests sets the stage for a rapid decline in conifer dominance during the 21st century. *Scientific Reports*, 8, 1–12. <https://doi.org/10.1038/s41598-018-24642-2>
- Shive, K., Preisler, H., Welch, K. R., Safford, H. D., Butz, R. J., O'Hara, K., & Stephens, S. L. (2018). Scaling stand-scale measurements to landscape-scale predictions of forest regeneration after disturbance: The importance of spatial pattern. *Ecological Applications*, 28, 1626–1639.
- Son, R., Wang, S. Y. S., Kim, S. H., Kim, H., Jeong, J. H., & Yoon, J. H. (2021). Recurrent pattern of extreme fire weather in California. *Environmental Research Letters*, 16, 094031. <https://doi.org/10.1088/1748-9326/ac1f44>
- Stan Development Team (2020). *RStan: The R interface to Stan*. <https://mc-stan.org/>
- State of California (2018). *California's 4<sup>th</sup> climate change assessment*. <https://www.climateassessment.ca.gov/state/index.html>
- State of California (2021). *California's wildfire and forest resilience action plan*. California Forest Management Task Force. <https://fmtf.fire.ca.gov/>
- Steel, Z. L., Foster, D., Coppoletta, M., Lydersen, J. M., Wing, B., Stephens, S. L., & Collins, B. M. (2021). Ecological resilience and vegetation transition in the face of multiple large wildfires. *Journal of Ecology*, 109, 3340–3355.
- Steel, Z. L., Koontz, M., & Safford, H. D. (2018). The changing landscape of wildfire: Burn pattern trends and implications for California's yellow pine and mixed conifer forests. *Landscape Ecology*, 33, 1159–1176. <https://doi.org/10.1007/s10980-018-0665-5>
- Steel, Z. L., Safford, H. D., & Viers, J. H. (2015). The fire frequency-severity relationship and the legacy of fire suppression in California forests. *Ecosphere*, 6(1), 1–23, Article 8. <https://doi.org/10.1890/ES14-00224.1>
- Stephens, S. L. (2005). Forest fire causes and extent on United States Forest Service lands. *International Journal of Wildland Fire*, 14(3), 213–222. <https://doi.org/10.1071/WF04006>
- Stephens, S. L., Collins, B. M., Fetting, C. J., Finney, M. A., Hoffman, C. M., Knapp, E. E., North, M. P., Safford, H., & Wayman, R. B. (2018). Drought, tree mortality, and wildfire in forests adapted to frequent fire. *BioScience*, 68, 77–88. <https://doi.org/10.1093/biosci/bix146>
- Stephens, S. L., Martin, R. E., & Clinton, N. E. (2007). Prehistoric fire area and emissions from California's forests, woodlands, shrublands, and grasslands. *Forest Ecology and Management*, 251, 205–216. <https://doi.org/10.1016/j.foreco.2007.06.005>
- Stephens, S. L., & Ruth, L. W. (2005). Federal forest-fire policy in the United States. *Ecological Applications*, 15, 532–542. <https://doi.org/10.1890/04-0545>
- Stevens, J. T., Collins, B. M., Miller, J. D., North, M. P., & Stephens, S. L. (2017). Changing spatial patterns of stand-replacing fire in California conifer forests. *Forest Ecology and Management*, 406, 28–36. <https://doi.org/10.1016/j.foreco.2017.08.051>
- Stewart, J. A. E., van Mantgem, P. J., Young, D. J. N., Shive, K. L., Preisler, H. K., Das, A. J., Stephenson, N. J., & Thorne, J. H. (2021). Influence of postfire climate and seed production on conifer regeneration. *Ecological Applications*, 31, e002280.
- Tepley, A. J., Thompson, J. R., Epstein, H. E., & Anderson-Teixeira, K. J. (2017). Vulnerability to forest loss through altered postfire recovery dynamics in a warming climate in the Klamath Mountains. *Global Change Biology*, 23, 4117–4132. <https://doi.org/10.1111/gcb.13704>
- Thompson, M. P., Bowden, P., Brough, A., Scott, J. H., Gilbertson-Day, J., Taylor, A., Anderson, J., & Haas, J. R. (2016). Application of wildfire risk assessment results to wildfire response planning in the southern Sierra Nevada, California, USA. *Forests*, 7(3), 64. <https://doi.org/10.3390/f7030064>
- USDA (2019). *Inyo National Forest Land and resource management plan*. USDA Forest Service, Pacific Southwest Region.
- Van de Water, K. M., & Safford, H. D. (2011). A summary of fire frequency estimates for California vegetation before Euroamerican settlement. *Fire Ecology*, 7(3), 26–58. <https://doi.org/10.4996/fireecology.0703026>
- van Wagtenonk, J. W. (2018). Fire as a physical process. In J. W. van Wagtenonk, N. G. Sugihara, S. L. Stephens, A. E. Thode, K. E. Shaffer, & J. Fites-Kaufman (Eds.), *Fire in California's ecosystems* (pp. 39–55). Univ of California Press.
- van Wagtenonk, J. W., & Lutz, J. A. (2007). Fire regime attributes of wildland fires in Yosemite National Park, USA. *Fire Ecology*, 3(2), 34–52. <https://doi.org/10.4996/fireecology.0302034>
- van Wagtenonk, J. W., Sugihara, N. G., Stephens, S. L., Thode, A. E., Shaffer, K. E., & Fites-Kaufman, J. (Eds.) (2018). *Fire in California's ecosystems*. Univ of California Press.
- Wahl, E. R., Zorita, E., Trouet, V., & Taylor, A. H. (2019). Jet stream dynamics, hydroclimate, and fire in California from 1600 CE to present. *Proceedings of the National Academy of Sciences of United States of America*, 116, 5393–5398. <https://doi.org/10.1073/pnas.1815292116>
- Welch, K. R., Safford, H. D., & Young, T. P. (2016). Predicting conifer establishment post wildfire in mixed conifer forests of the North American Mediterranean-climate zone. *Ecosphere*, 7(12), e01609.
- Westerling, A. L., Hidalgo, H. G., Cayan, D. R., & Swetnam, T. W. (2006). Warming and earlier spring increase western US forest wildfire activity. *Science*, 313, 940–943.
- Young, D., Meyer, M., Estes, B., Gross, S., Wuenschel, A., Restaino, C., & Safford, H. D. (2020). Forest recovery following extreme drought in California, USA: Natural patterns and effects of pre-drought management. *Ecological Applications*, 30, e02002.
- Young, D. J. N., Stevens, J. T., Earles, J. M., Moore, J., Ellis, A., Jirka, A. L., & Latimer, A. M. (2017). Long-term climate and competition explain forest mortality patterns under extreme drought. *Ecology Letters*, 20, 78–86. <https://doi.org/10.1111/ele.12711>
- Zhou, X., Josey, K., Kamareddine, L., Caine, M. C., Liu, T., Mickley, L. J., Cooper, M., & Dominici, F. (2021). Excess of COVID-19 cases and deaths due to fine particulate matter exposure during the 2020 wildfires in the United States. *Science Advances*, 7(33), p.eabi8789. <https://doi.org/10.1126/sciadv.abi8789>



**BIOSKETCH**

**HUGH D. SAFFORD** is Chief Scientist of Vibrant Planet and a member of the research faculty in the Department of Environmental Science and Policy at the University of California, Davis. He was the Regional Ecologist for the Pacific Southwest Region of the USDA Forest Service until his retirement on 30 December 2021. His research interests focus on fire and vegetation ecology, ecological restoration, science translation and support to resource management.

**SUPPORTING INFORMATION**

Additional supporting information may be found in the online version of the article at the publisher's website.

**How to cite this article:** Safford, H. D., Paulson A. K., Steel Z. L., Young D. J. N., & Wayman R. B. (2022). The 2020 California fire season: A year like no other, a return to the past or a harbinger of the future? *Global Ecology and Biogeography*, 00, 1–21. <https://doi.org/10.1111/geb.13498>